A New Analysis of Photospheric Fields and Flows

Brian T. Welsch
Space Sciences Laboratory, University of California, Berkeley

Magnetic evolution observed in high-cadence sequences of high-resolution, seeing-free magnetograms of the photosphere by Hinode (and of the chromosphere by Solar-C) can constrain the dynamics of near-surface magnetic and velocity fields. Such observations can address open questions about several key topics in solar physics, including coronal heating, flux emergence and submergence, and impulsive magnetic dynamics in flares. I will discuss research ideas in these and other subject areas.

Personal outlook: In theory, we will be happier if we learn to be content – a Zen-like view.

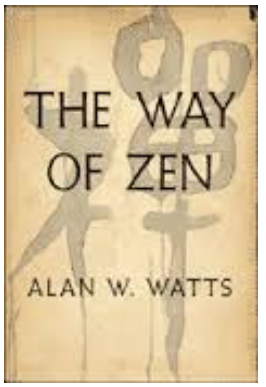

As a teenager, my world view was strongly influenced by Alan Watts' *The Way of Zen*.

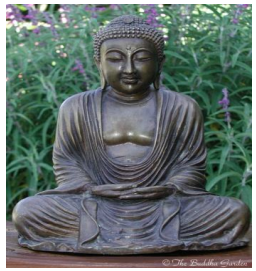

One idea: accept the world "is what it is"– not what we want it to be! So: **be content**.

But while Zen theory sounded good to me, Zen practice sounded painful!

keisaku "nudge"

So I never learned to be content –
and now I always want **new observations!**

Topical Outline

1. **Coronal heating:** Are rapidly evolving flows present to drive Alfvénic turbulence for coronal heating?

2. **Flux emergence and submergence:** To what extent are these non-ideal processes?

3. **Field evolution in flares:** How do photospheric & chromospheric fields change in flares?

Format of Discussion:

- First, what can be learned with ***current*** observational capabilities?

- Second, what could be learned with improved observational capabilities?
  - resolution of smaller length scales
  - observations at multiple heights

Starting point: Faraday's & Ohm's laws imply that **v** is related to field evolution $\partial_t \mathbf{B}$ in magnetogram sequences.

The ideal induction equation relates **v** to $\partial_t \mathbf{B}$,

$$\partial_t \mathbf{B} = -c(\nabla \times \mathbf{E}) = \nabla \times (\mathbf{v} \times \mathbf{B})$$

assuming the ideal Ohm's law applies,* relating **v** to **E** via

$$\mathbf{E} = -(\mathbf{v} \times \mathbf{B})/c$$

*One could instead use **E** = -(**v** x **B**)/c + **R**, if some *known* resistivity **R** is assumed.

Why do we care about v or E? Photospheric flow fields (or electric fields $\mathbf{E}_{ph}$) can quantify aspects of evolution in $\mathbf{B}_{cor}$.

- The fluxes of magnetic **energy** & **helicity** across the magnetogram surface into the corona depend upon $\mathbf{E}_{ph}$:

$$dU/dt = \int dA \, (\mathbf{B}_{ph} \times [\mathbf{v}_{ph} \times \mathbf{B}_{ph}])_z \, /4\pi$$
$$dH/dt = 2 \int dA \, (\mathbf{A}_{ph} \times [\mathbf{v}_{ph} \times \mathbf{B}_{ph}])_z$$

  U and *H* probably play central roles in coronal heating, flares, and CMEs.

- Coupling of $\mathbf{B}_{cor}$ to $\mathbf{B}_{ph}$ also implies that $\mathbf{E}_{ph}$ provides **boundary conditions** for **data-driven,** time-dependent simulations of $\mathbf{B}_{cor}$ (e.g., Cheung & DeRosa 2012).

The electric field **E** can be estimated from magnetic evolution $\partial_t \mathbf{B}$, via Faraday's law: $\partial_t \mathbf{B} = -c(\nabla \times \mathbf{E})$.

Vector **B** in AR 8210:

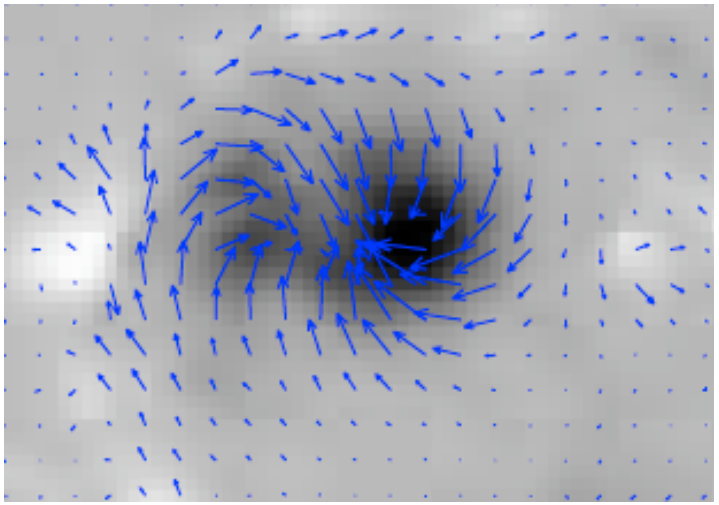

The part of $\mathbf{B}_h$ due only to J_z:

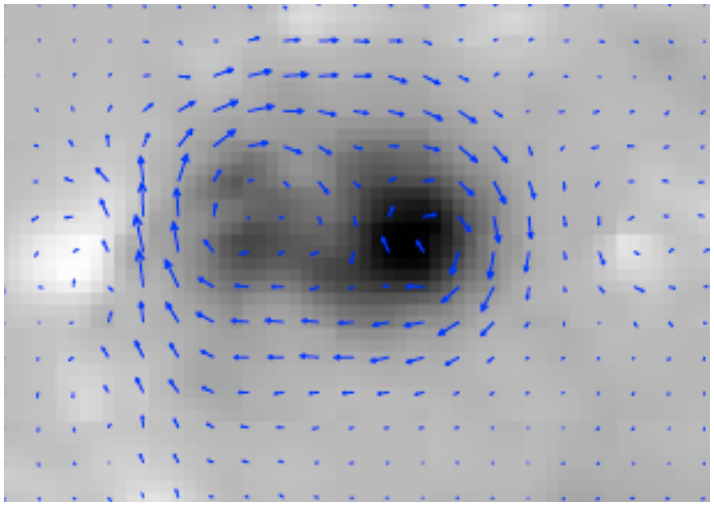

Express **B** in divergence-free form:

$$\mathbf{B} = \nabla \times (\nabla \times \mathcal{B}\hat{\mathbf{z}}) + \nabla \times \mathcal{J}\hat{\mathbf{z}}$$

$$\Longrightarrow \partial_t \mathbf{B} = \nabla \times (\nabla \times \partial_t \mathcal{B}\hat{\mathbf{z}}) + \nabla \times \partial_t \mathcal{J}\hat{\mathbf{z}}$$

Next, solve: $\nabla_h^2(\partial_t \mathcal{B}) = \partial_t B_z$

$$\nabla_h^2(\partial_t \mathcal{J}) = 4\pi \partial_t J_z / c$$

Apply Faraday's law:

$$\mathbf{E} = (\nabla \times \partial_t \mathcal{B}\hat{\mathbf{z}}) + \partial_t \mathcal{J}\hat{\mathbf{z}} - \nabla\psi$$

NB: ψ is not unconstrained by $\partial_t \mathbf{B}$, so use Ohm's law, tracking, Doppler…

Fisher et al. 2010

Applying Faraday's law only partially determines **E**!

Note that:

$\partial_t \mathbf{B}_h$ also depends upon **vertical derivatives** in $\mathbf{E}_h$, which **single-height** magnetograms do not fully constrain.

But also note:

Faraday's law only relates $\partial_t \mathbf{B}$ to the **curl** of **E**, not **E** itself; a "gauge electric field" $\nabla\psi$ is unconstrained by $\partial_t \mathbf{B}$.

==> Multiple-height magnetograms from Solar C will help, but not completely solve this problem!

Additional constraints: Ohm's law; **v** from tracking; Doppler data.

NB: The non-inductive part of **E** is very important!

- The inductive field $\mathbf{E}_{ind}$, by itself, does ***not*** closely match the actual **E** in tests using MHD "data."
- **Progress**: Several approaches to better constrain $\nabla\psi$ have already been investigated:

$$c\mathbf{E}_{tot} = \underbrace{c\mathbf{E}_{ind}}_{\text{PTD(inductive) solution}} \underbrace{-\nabla_h\psi_{Dopp}}_{\text{Doppler constraint}} \underbrace{-\nabla_h\psi_{FLCT}}_{\text{Tracking constraint}} \underbrace{-\nabla\psi}_{\text{Additional free potential function}} \underbrace{-\nabla\psi_{Ohm}}_{\text{Ideal Ohm's aw}}$$

Non-inductive constraints

The second and third right-side terms represent non-inductive contributions from Doppler shifts and pattern motions (derived from e.g. FLCT or DAVE), respectively, from which the inductive contributions have been removed. Additional constraints can be imposed, represented by the fourth term. The fifth term, imposed as a final step, enforces the condition $\mathbf{E}_{tot}\bullet\mathbf{B} = 0$.

See Fisher et al. 2012, Sol. Phys. 277, p153 for more details.

And there are other problems: Observations give us $\Delta\mathbf{B}/\Delta t$, not $\partial_t\mathbf{B}$; and spatial resolution is limited.

Hence, $\partial_t\mathbf{B} = -c(\nabla \times \mathbf{E}) = \nabla \times (\mathbf{v} \times \mathbf{B})$ becomes, at ***best***:

$$\Delta\mathbf{B}/\Delta t = -c(\nabla \times \langle\mathbf{E}\rangle) = \nabla \times (\langle\mathbf{v}\rangle \times \langle\mathbf{B}\rangle + \langle\mathbf{v} \times \mathbf{B}\rangle)$$

where $\langle,\rangle$ denote convolution over spatial & temporal resolution. (This also ignores errors in measured **B**!)

And it can get worse: estimating **v** by tracking yields ***further*** spatial averaging over the "apodization" window!

Fourier local correlation tracking (FLCT) finds **v**(x, y) by correlating evolution in **regions** to find local shifts.

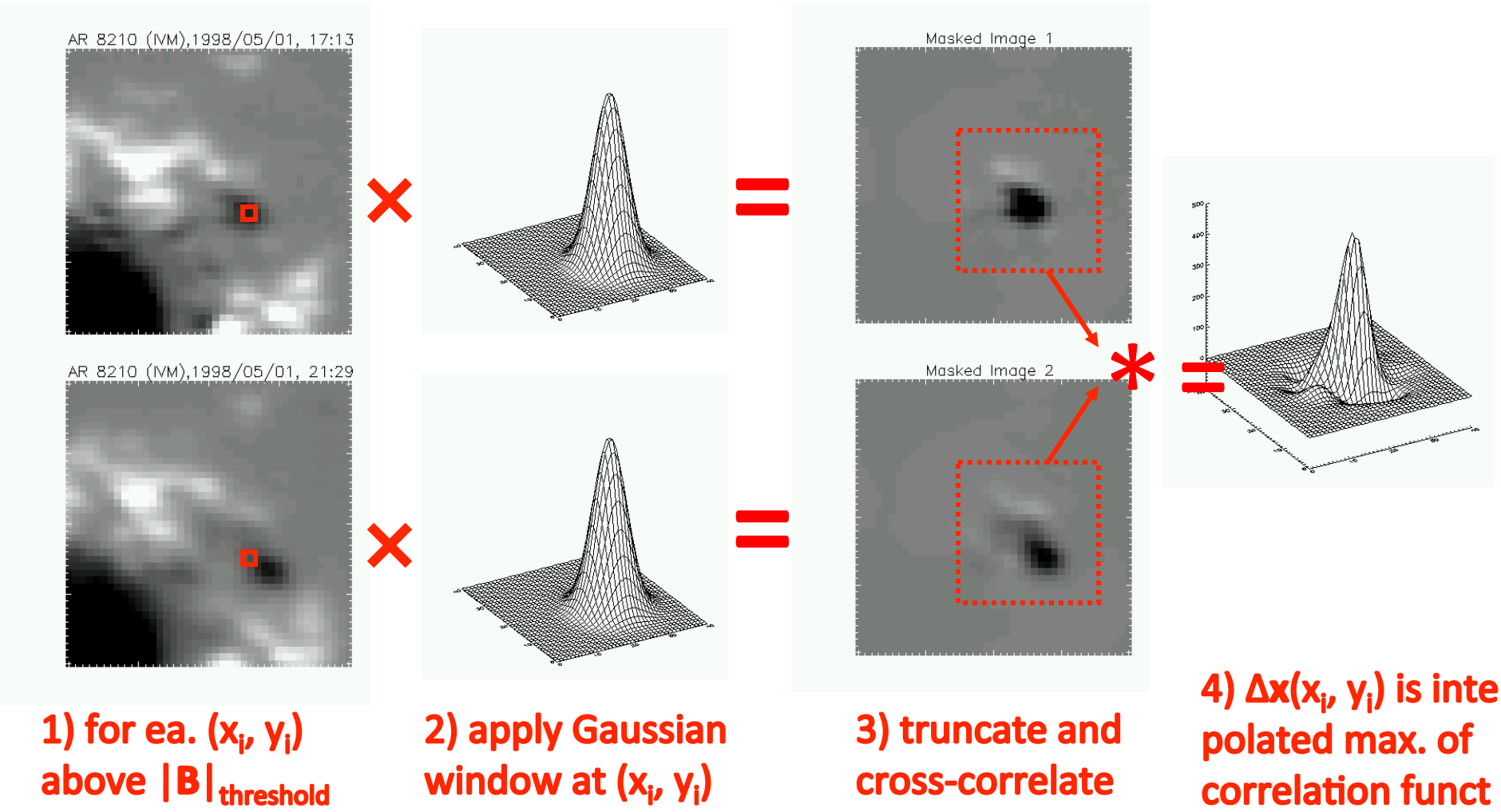

1) for ea. (x_i, y_i) above $|B|_{threshold}$

2) apply Gaussian window at (x_i, y_i)

3) truncate and cross-correlate

4) $\Delta x(x_i, y_i)$ is interpolated max. of correlation funct

Windowing implies spatial averaging of the underlying flow field.

LCT can track sequential images of ***almost anything*** (e.g., coronal fans by McKenzie et al.) to find **v**(x, y).

Hathaway et al. (2013, *Science,* in press) tracked the pattern of supergranular cells to detect "banana" cells.

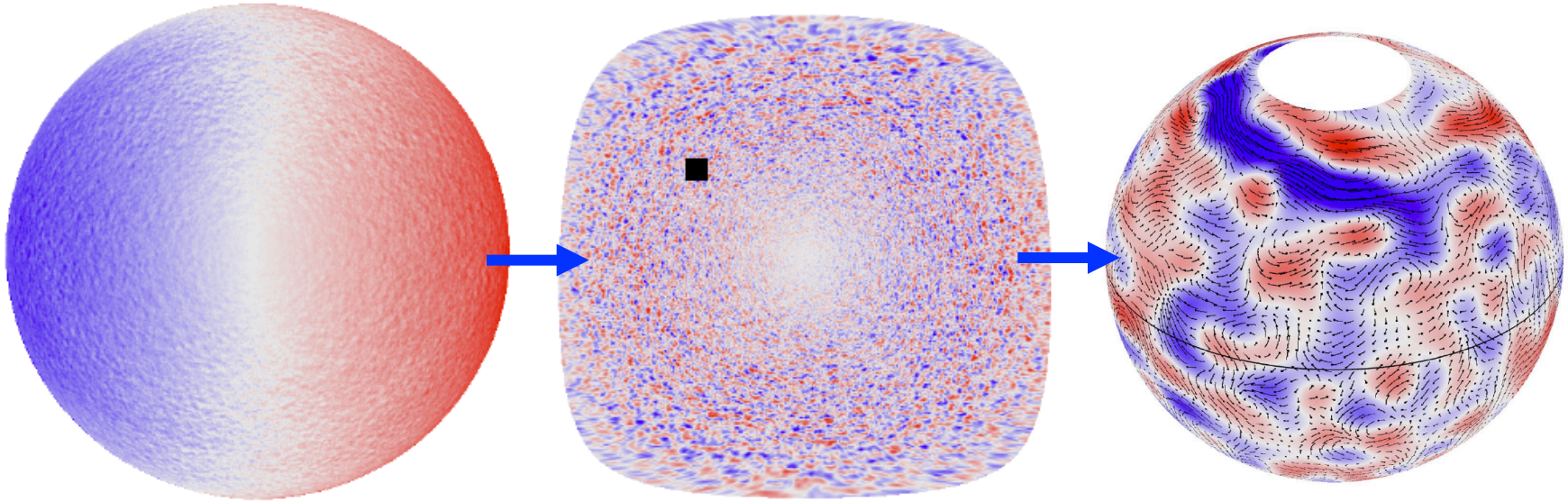

Remove rotation, meridional flow, & reproject.

Supergranules act as tracers of larger-scale **v**.

Topic 1: van Ballegooijen et al. (2011) suggest convection drives Alfvénic turbulence to heat the chromosph. & corona.

The Astrophysical Journal, 736:3 (27pp), 2011 July 20

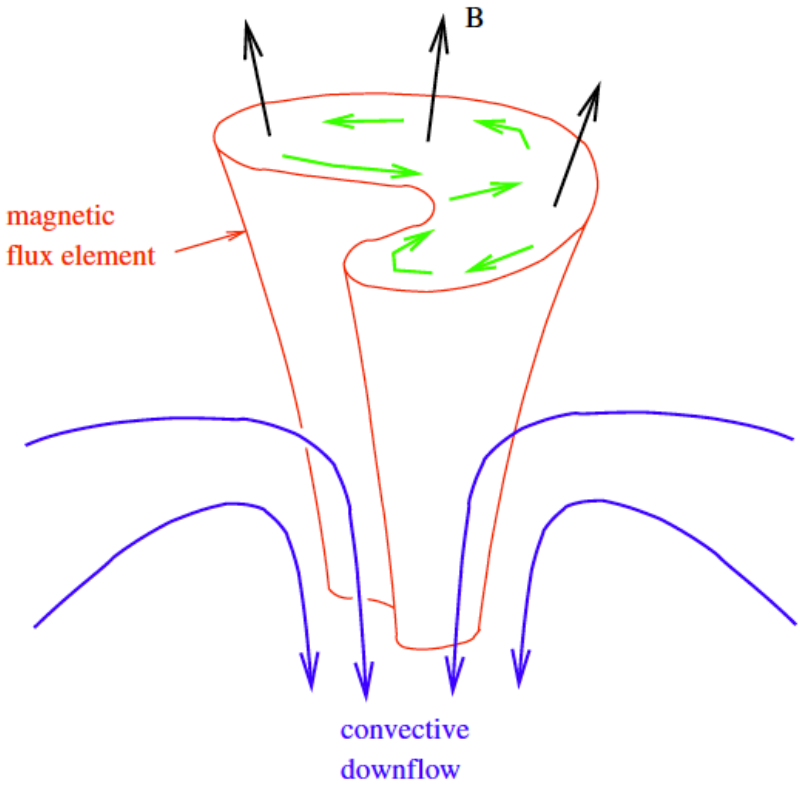

Figure 1. Interaction of a magnetic flux element with convective flows in an intergranular lane. The red object indicates the magnetic element containing a nearly vertical magnetic field, as indicated by the black arrows. The blue arrows indicate the convective flow, which push on the flux tube from one side. Due to the stiffness of the magnetic field, horizontal momentum is transported upward, which results in a distortion of the shape of the flux tube and generates transverse motions inside it (green arrows). We suggest these transverse motions create Alfvén waves that propagate into the upper atmosphere.

Motions must be:

1. rapid,
   v_{ph} = 1-2 km/sec
2. small-scale,
   L < 100 km
3. rapidly varying,
   $\tau_{\text{flow life}}$ = 60 -- 200 sec

Welsch et al. (2012) investigated **flow lifetimes** at various spatial scales in *Hinode*/SOT/NFI observations of AR 10930.

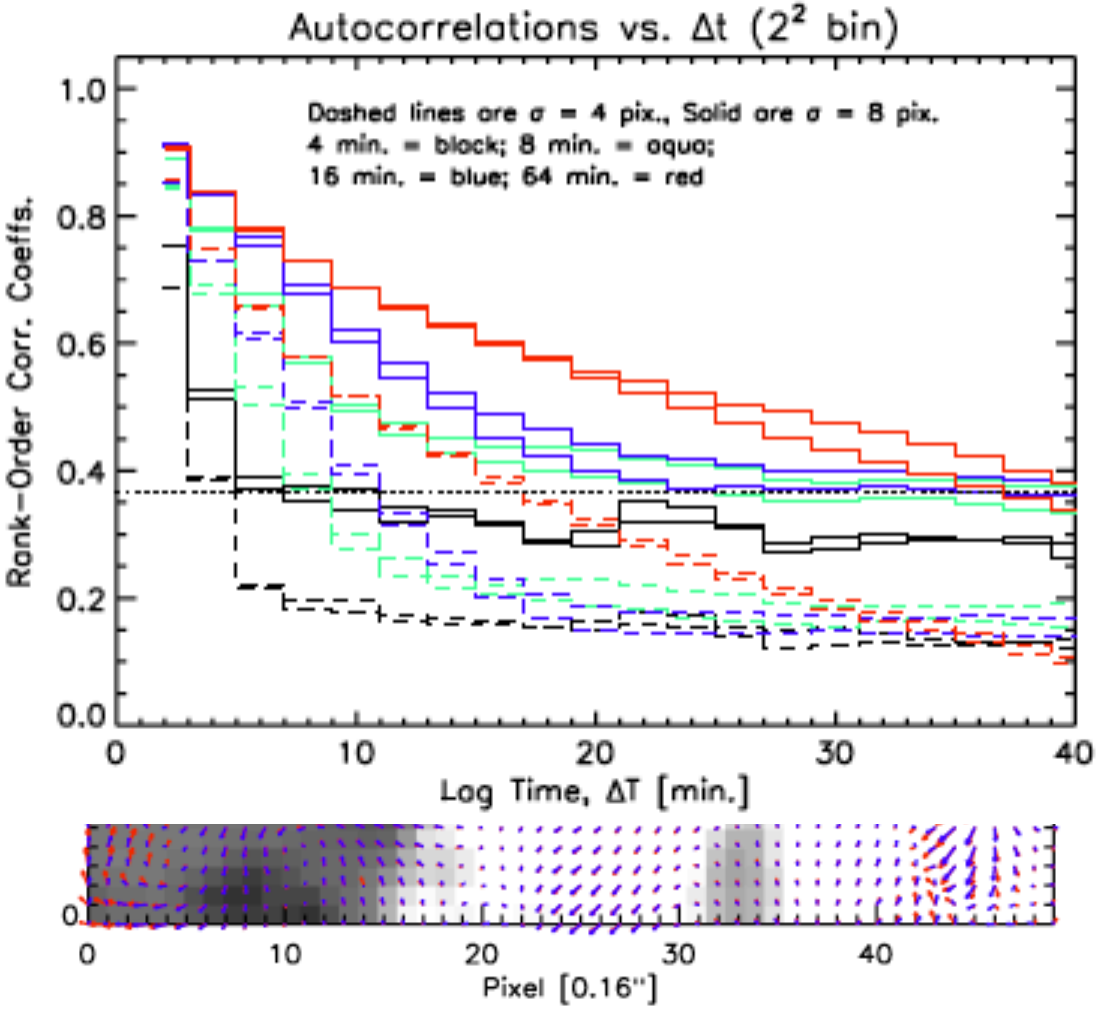

- B_{LoS} in "line-wing" magnetograms
- cadence ≈ 120 sec for 13 hr.
- magnetogram pixels binned to 0''.3

We estimated flow lifetimes by autocorrelating maps of flow components (v_x, v_y) in subregions of the active region.

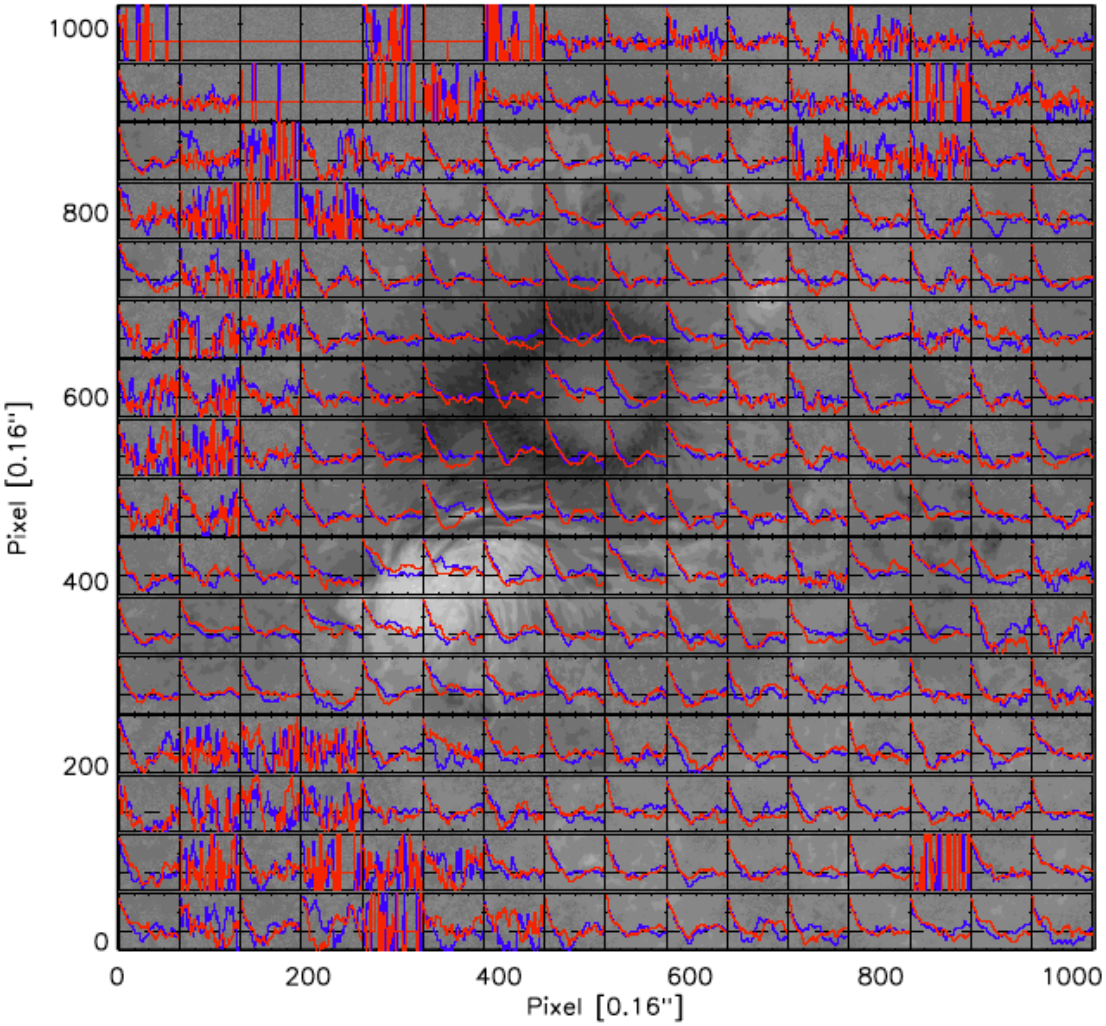

Lifetime τ was found by fitted autocorrelation with $e^{-t/\tau}$.

We found that flows are faster at smaller spatial scales…

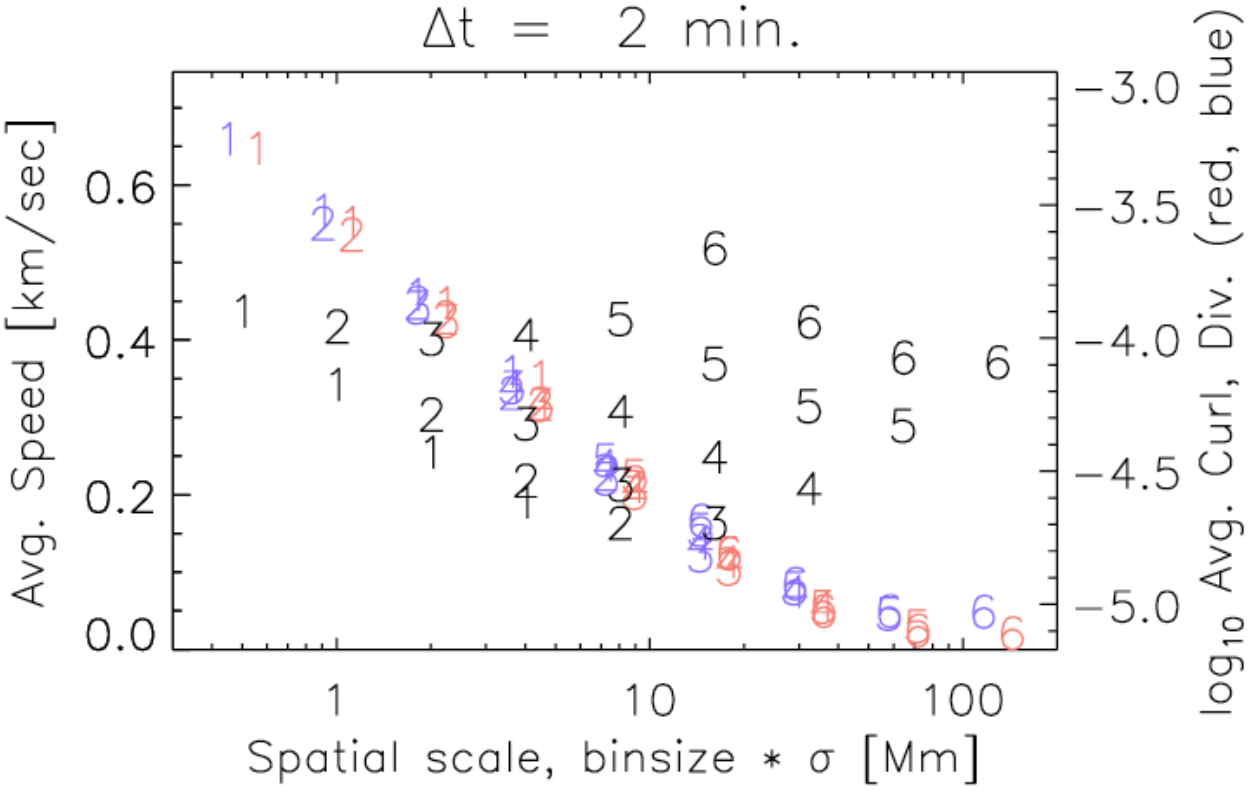

Smallest scale resolved is c. 500 km

Extrapolating, speeds at 50 km would be 1 km sec.

Average speeds inferred from tracking, as a function of spatial scale (pixel binning x windowing parameter): **flows on smaller scales are faster.**

Note: magnetic fields inhibit convection, so flows in magnetized regions are smaller than in field-free regions.

Lifetimes of magnetic structures, from autocorrelation, are longer in regions with higher field strengths.

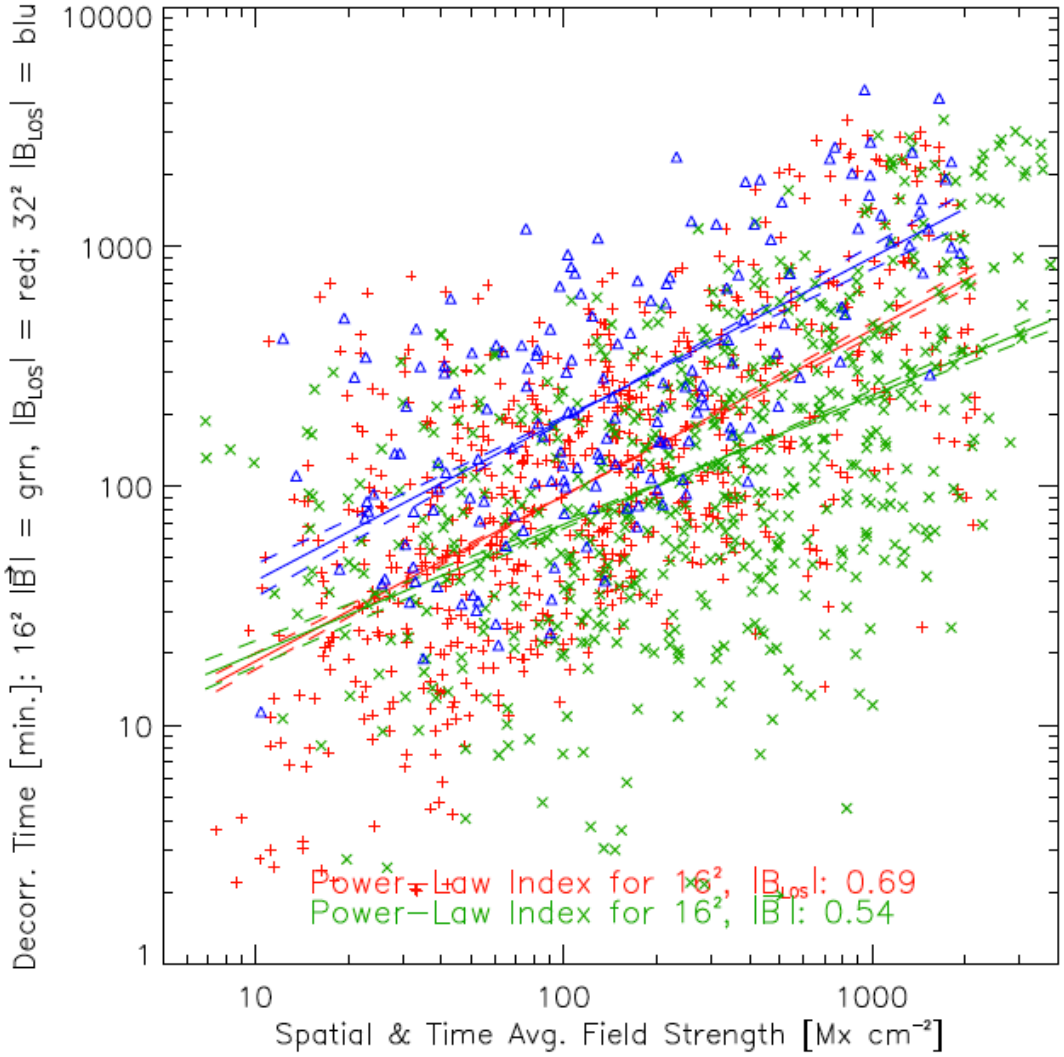

This trend is true for B_{LOS}, B_z, and $|B|$.

This is consistent with strong fields inhibiting convective flows.

Lifetimes of velocities, from autocorrelation of flow maps, are also longer in regions with higher field strengths.

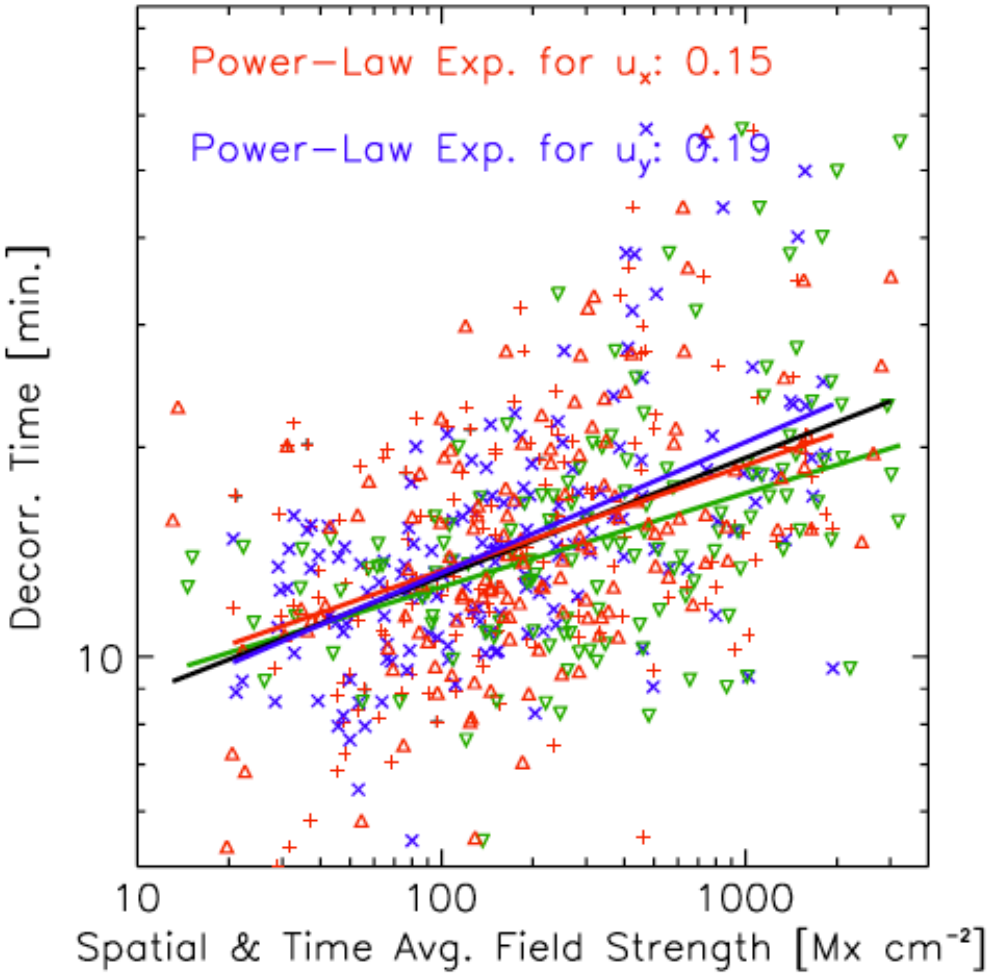

This trend is true for B_{LoS}, B_z, and $|B|$.

Lorentz forces – which persist as long as **B** does! – probably partly govern flow evolution in strong fields.

We found that flows are faster at smaller spatial scales…
…and that faster flows are shorter-lived.

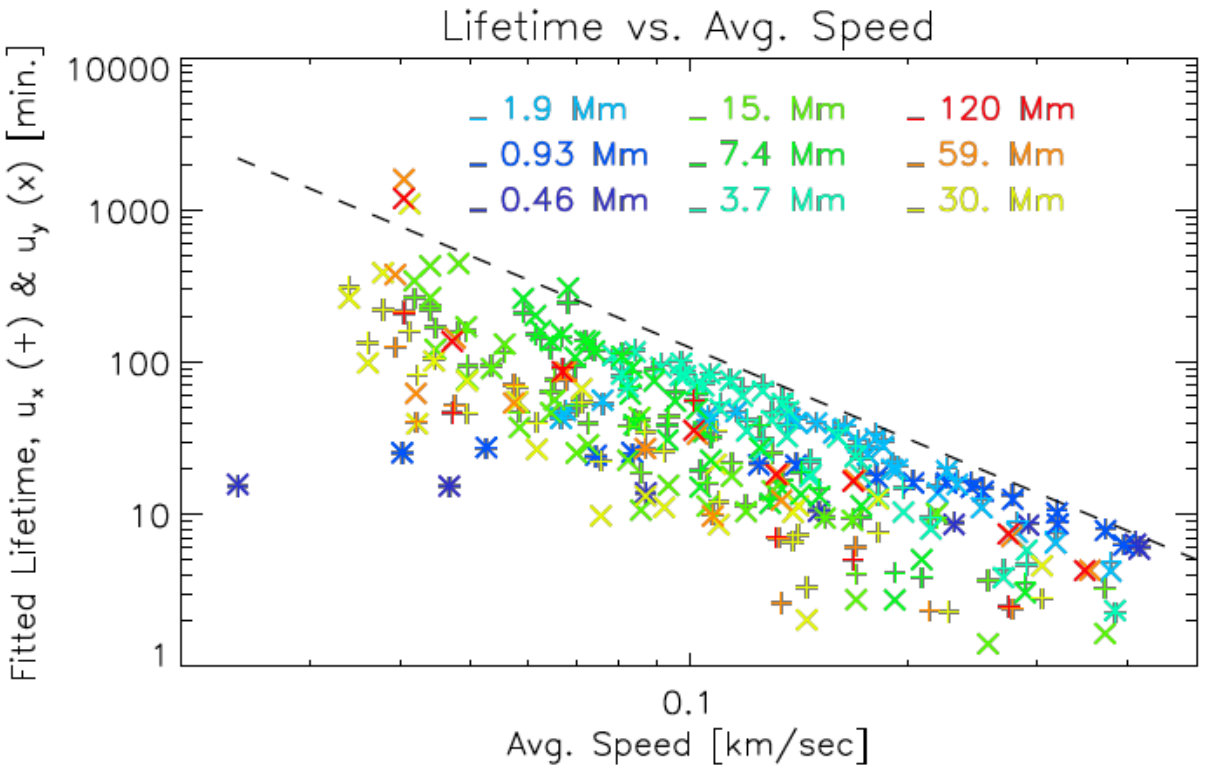

Max. flow lifetimes scale as $\tau_{life} \propto (1/v_0^2)$

Extrapolation to speeds near 1 km/sec implies peak lifetimes of 3-5 min.

Fitted lifetime (assuming exponential decay) vs. flow speed, for flows on a range of spatial scales: **higher average speeds correspond to shorter lifetimes.**

Extrapolated results from *Hinode*/SOT suggest flow lifetimes are too long for van Ballegooijen et al.'s model.

We found that flows are faster at smaller spatial scales…
…and that they are also shorter-lived.

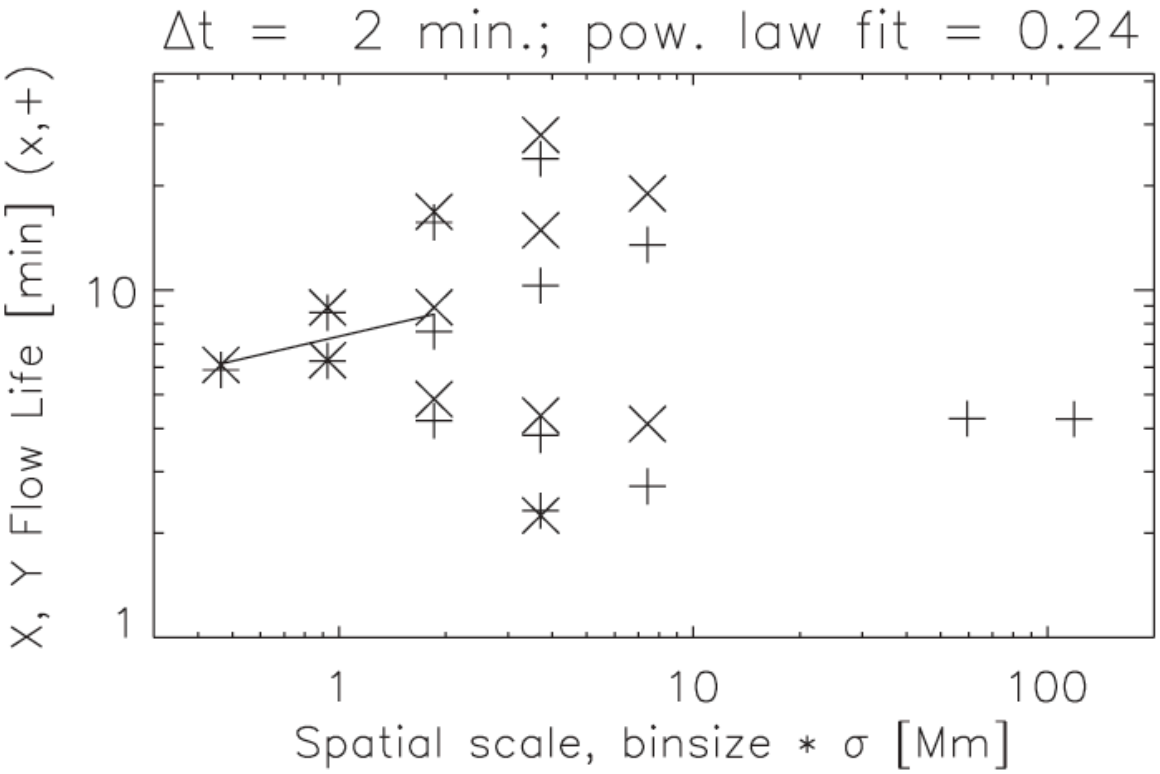

Extrapolation to scales of 50 km implies flow lifetimes of 5 min.

Fitted lifetime (assuming exponential decay) vs. spatial scale of inferred flow (window x binning): **smaller-scale flows tend to have shorter lifetimes.**

Extrapolated results from *Hinode*/SOT suggest flow lifetimes are **too long** for van Ballegooijen et al.'s model.

Conclusion 1: Clearly, higher-resolution studies of flow lifetimes in magnetic regions are needed.

- The target resolution of Solar-C's SUVIT, < 0''.1, matches hypothesized scale, so will be helpful.

- Unfortunately, windowing used in tracking (e.g., Bonet et al. 2010) lowers effective resolution.

- ATST's target resolution, near 0''.03, will help characterize lifetimes of the smallest-scale flows.

<u>Topic 2:</u> Flux emergence & submergence play crucial roles in solar activity. Are electric fields in these processes ideal?

Pariat et al. 2004

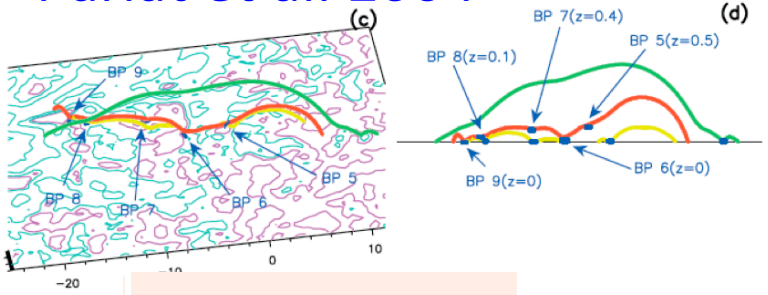

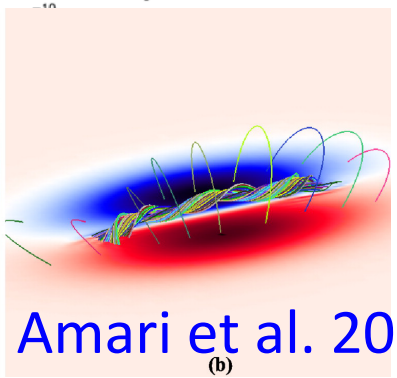

Amari et al. 2003

- Is reconnection ***<u>required</u>*** for new magnetic flux to emerge?
- Does non-ideal "cancellation" form coronal flux ropes that are CME precursors?
- Is the removal each solar cycle's photospheric flux non-ideal?

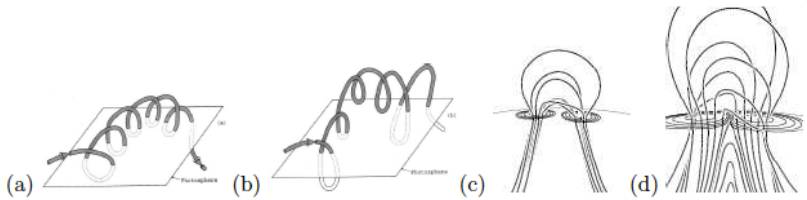

Low 2001

van Ballegooijen et al. 2008

Pariat et al. (2004), *Resistive Emergence of Undulatory Flux Tubes*:

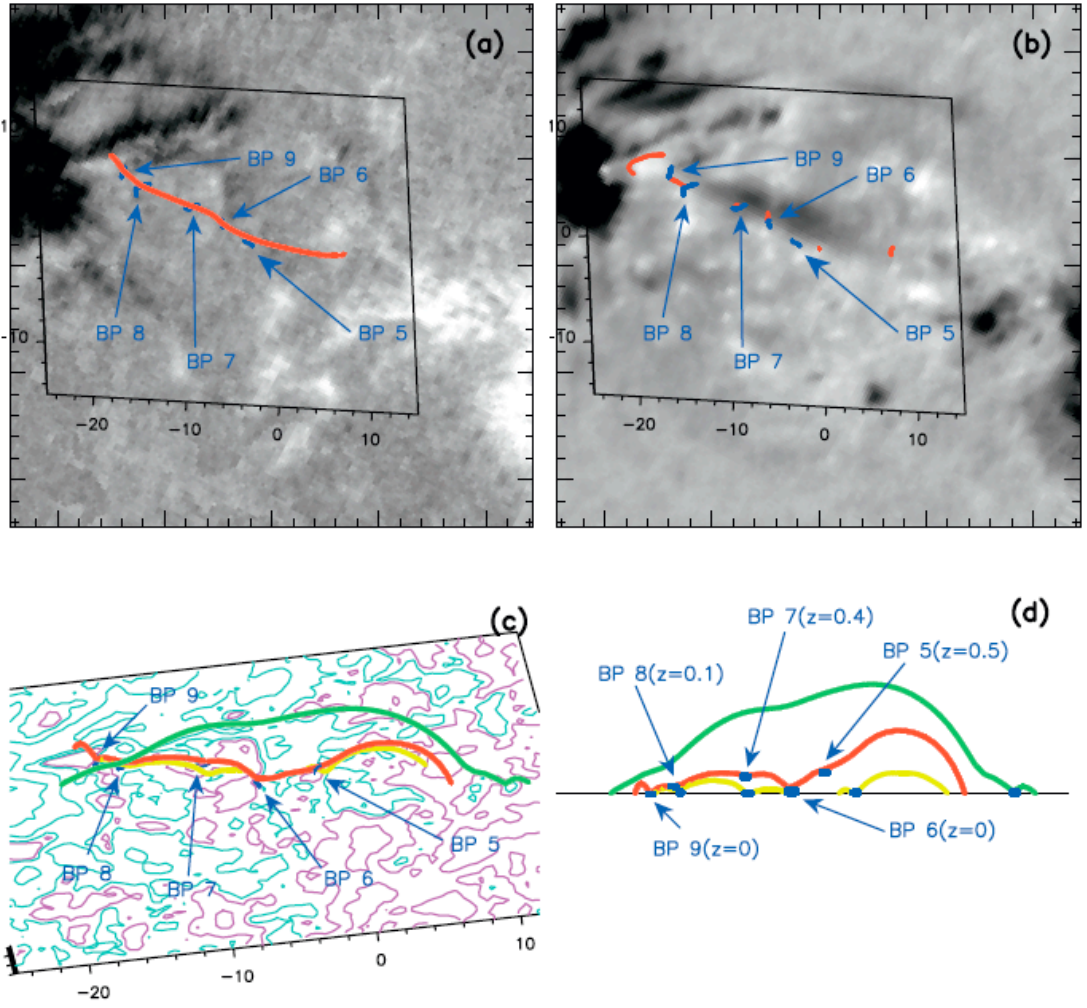

"These findings suggest that arch filament systems and coronal loops do not result from the smooth emergence of large-scale Ω-loops from below the photosphere, but rather from the rise of undulatory flux tubes whose upper parts emerge because of the Parker instability and **whose dipped lower parts emerge because of magnetic reconnection**.

Ellerman Bombs are then the signature of this resistive emergence of undulatory flux tubes."

PILs are special: Flux ***only*** emerges or submerges along polarity inversion lines (PILs) of the radial magnetic field.

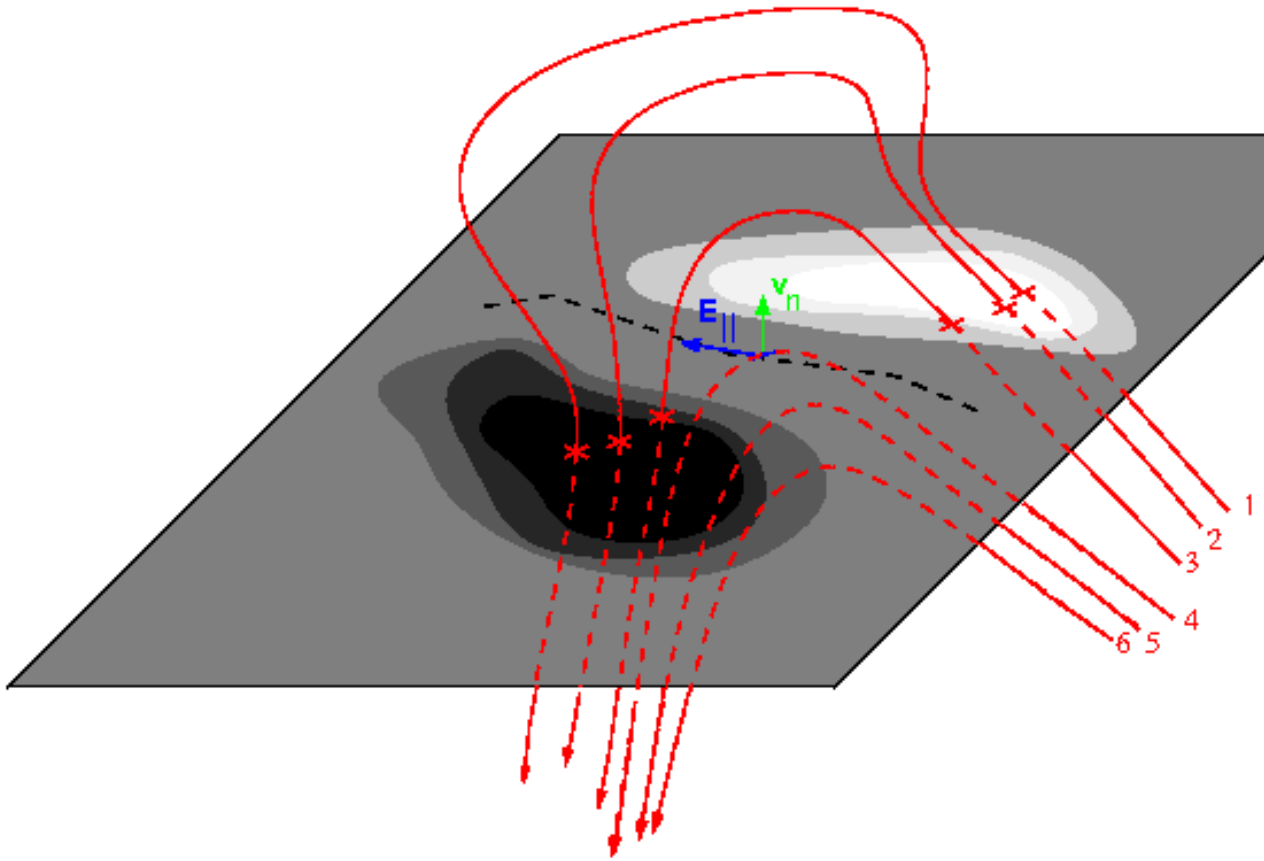

Along PILs of B_r, field lines osculate the photosphere (i.e., are tangent at PIL points).

Via Faraday's law, emergence / submergence requires an electric field E_h along PILs.

Changes in LOS flux should match Doppler velocities on PILs multiplied by transverse field strengths.

From LOS m'gram: $$\frac{\Delta\Phi_{\mathrm{LOS}}}{\Delta t} = \frac{1}{2}\sum_{\text{near PIL}} \Delta x^2 \left[\left| B_{\mathrm{LOS}}(t_f) \right| - \left| B_{\mathrm{LOS}}(t_i) \right| \right]$$

From Faraday's law, $$\frac{\Delta\Phi}{\Delta t} = -c\int da\,(\nabla\times\mathbf{E})\cdot\hat{\mathbf{n}} = \int da\,(\nabla\times(\mathbf{v}\times\mathbf{B}))\cdot\hat{\mathbf{n}}$$

Since flux can only emerge or submerge at a PIL,

$$\frac{\Delta\Phi_{\mathrm{PIL}}}{\Delta t} = \sum_{\mathrm{PIL}} \mathrm{dx}\ \hat{l}\cdot(\mathbf{v}_{\mathrm{LOS}}\times\mathbf{B}_{\mathrm{transverse}})$$

Summed Dopplergram and transverse field along PIL pixels.

In the absence of errors, $\Delta\Phi_{\mathrm{LOS}}/\Delta t = \Delta\Phi_{\mathrm{PIL}}/\Delta t$.

Aside: Flows $v_{||}$ along **B** do not contribute to **E** = -(**v** x **B**)/c, but do "contaminate" Doppler measurements.

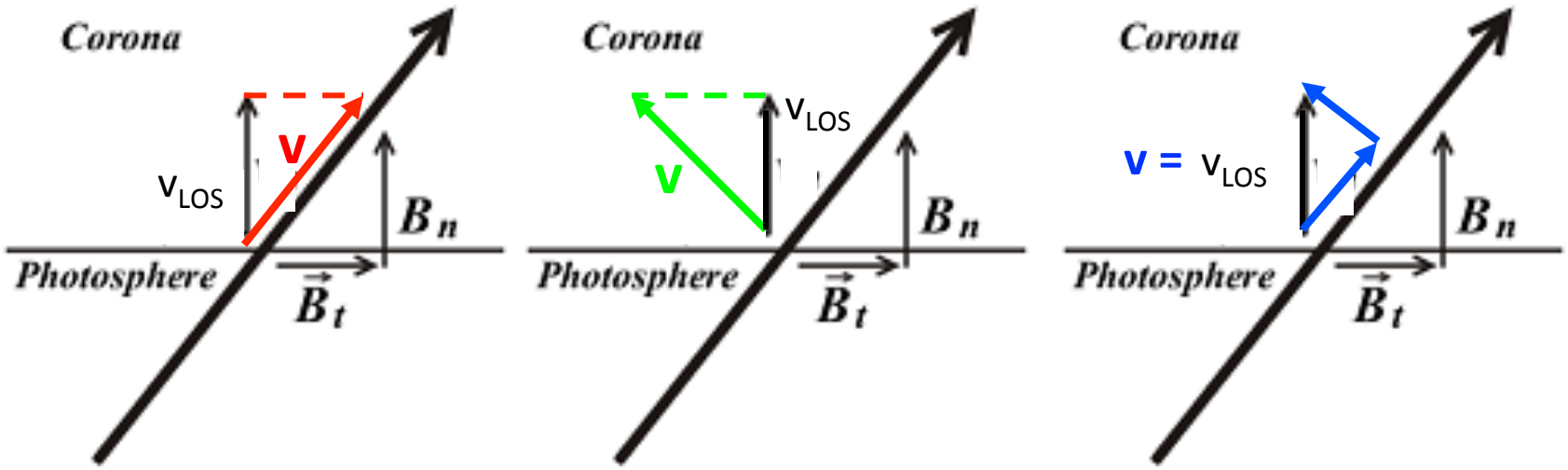

Generally, Doppler shifts cannot distinguish flows parallel to **B** **(red)**, perpendicular to **B** **(green)**, or in an intermediate direction **(blue)**.

With $\mathbf{v}_{\perp}$ estimated another way & projected onto the LOS, the Doppler shift determines $v_{||}$ (Georgoulis & LaBonte 2006).

Doppler shifts are **only** unambiguous along polarity inversion lines (PILs), where B_n changes sign (Chae *et al*. 2004, Lites 2005).

Ideally, change in LOS flux $\Delta\Phi_{LOS}/\Delta t$ should match flux change $\Delta\Phi_{PIL}/\Delta t$ from vertical flows transporting $\boldsymbol{B}_h$ across the PIL (black dashed line).

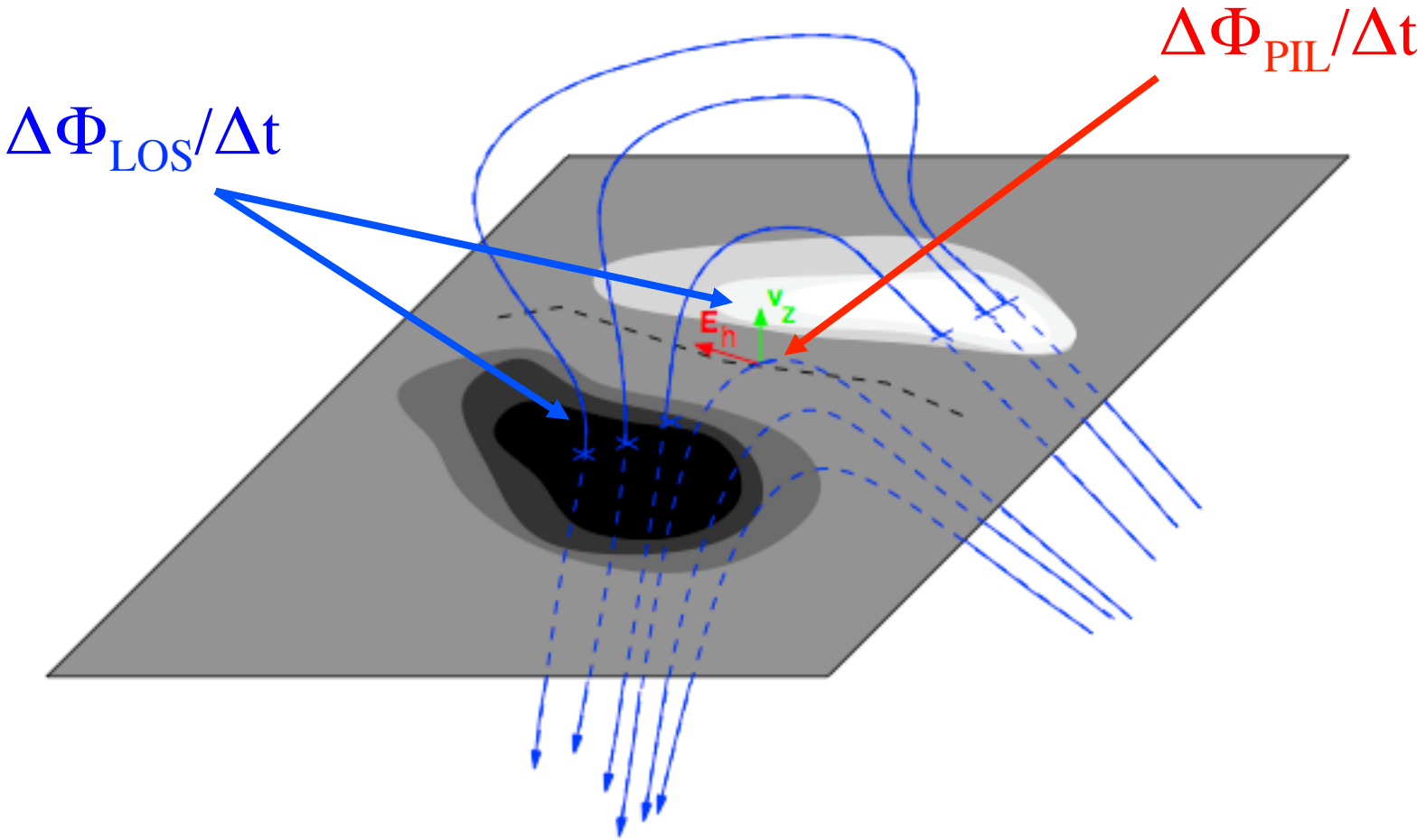

NB: The analysis here applies only near disk center!

Important magnetodynamics is not always apparent in $\Delta B_z/\Delta t$ near PILs -- e.g., flux emergence!

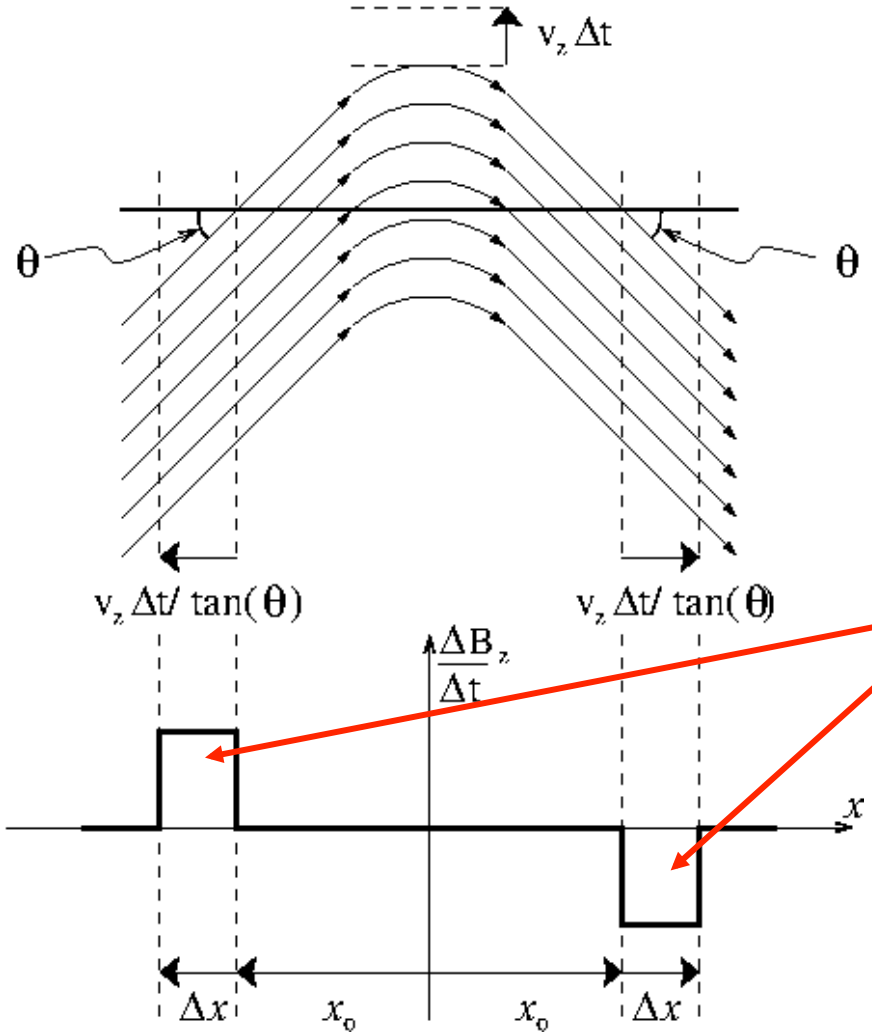

This sketch of flux emergence in a bipolar magnetic region shows the emerging field viewed in cross-section normal to the polarity inversion line (PIL).

Note the strong signature of the field change at the edges of the region, while the change in photospheric field at the PIL is zero.

ASIDE: Because magnetic fields suppress convection, magnetized regions have *pseudo-redshifts*, as on these PILs.

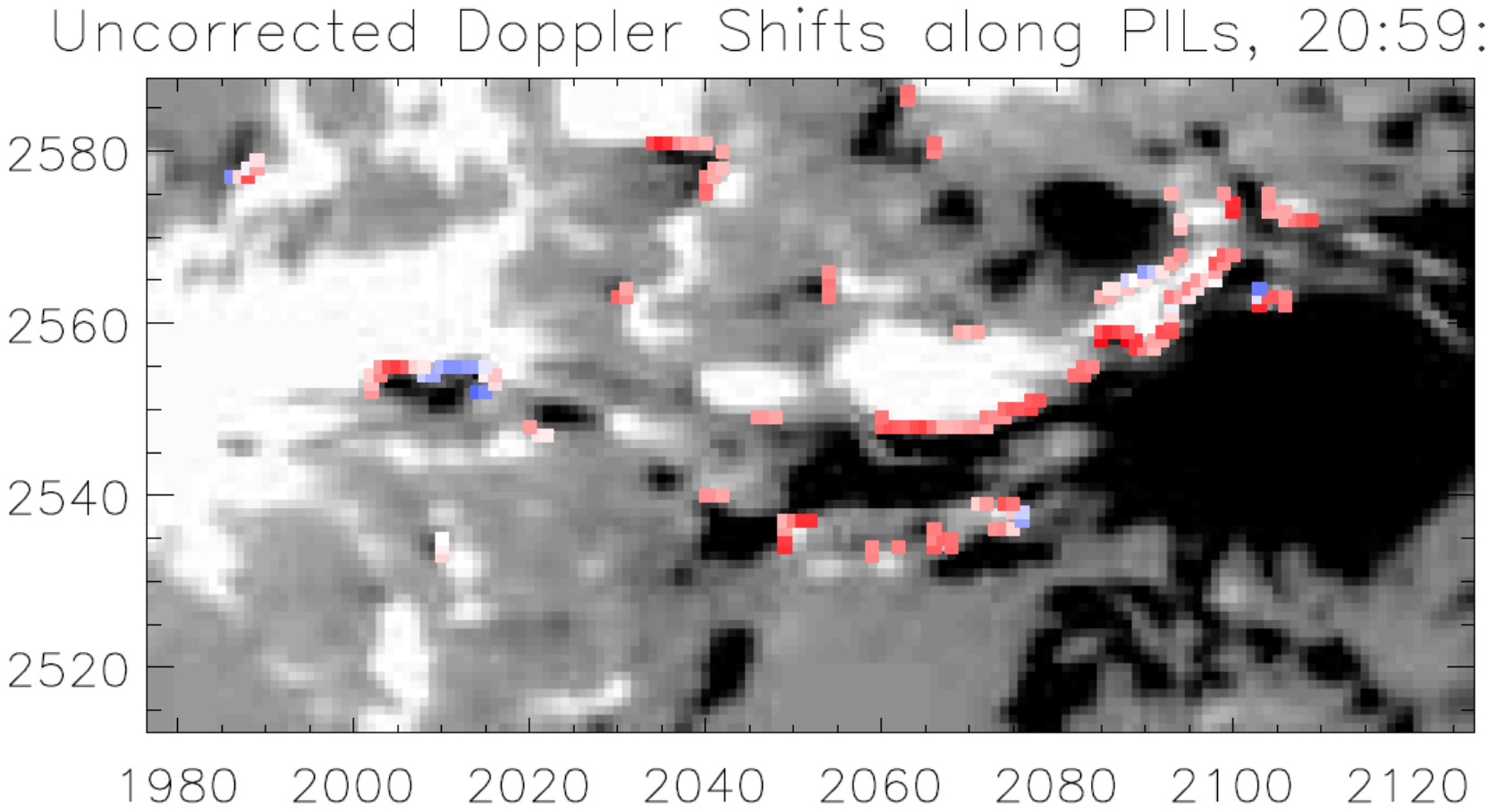

Here, an automated method (Welsch & Li 2008) identified PILs in a subregion of AR 11117, color-coded by Doppler shift.

HMI Doppler observations show blueshifts along PILs, associated with flux emergence (Welsch et al. 2013).

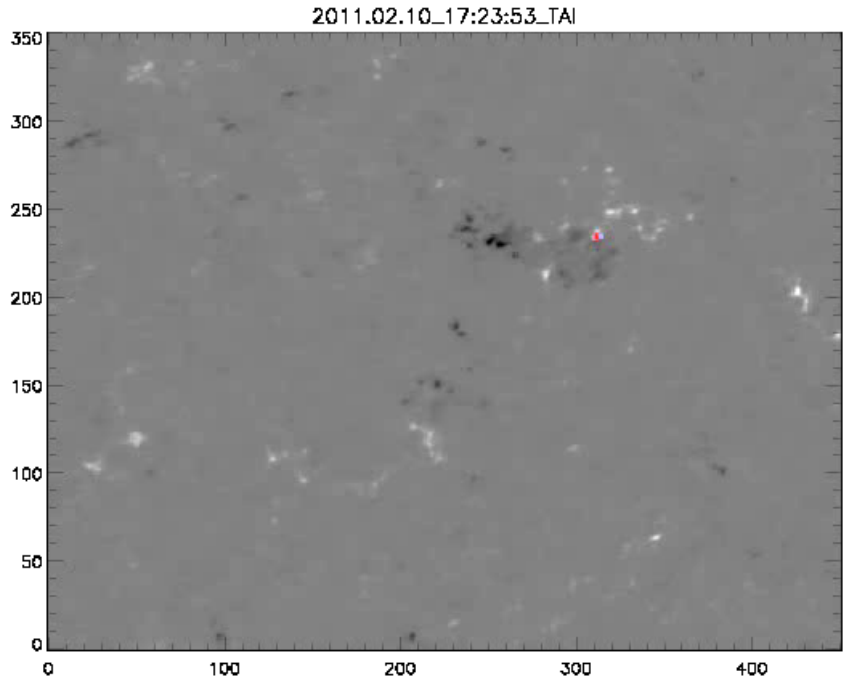

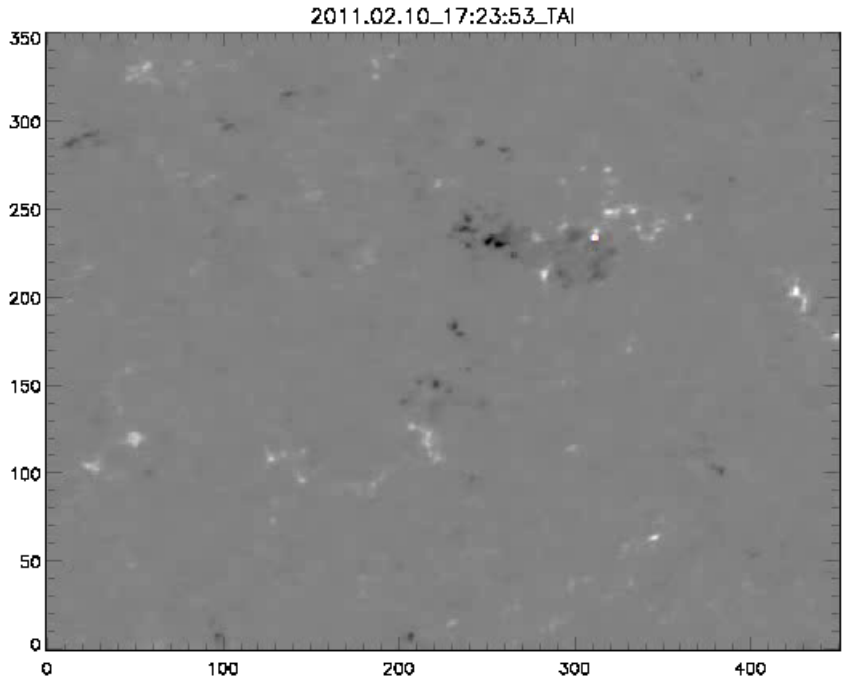

Left: Raw Doppler shifts on LOS PILs in AR 11158.
Note "false" PILs in penumbrae, with evershed flow.

Right: Doppler shifts with convective blueshift removed, on PILs of B_{LOS} near PILs of B_r.

Distinct physical processes can underlie increases or decreases in magnetic flux.

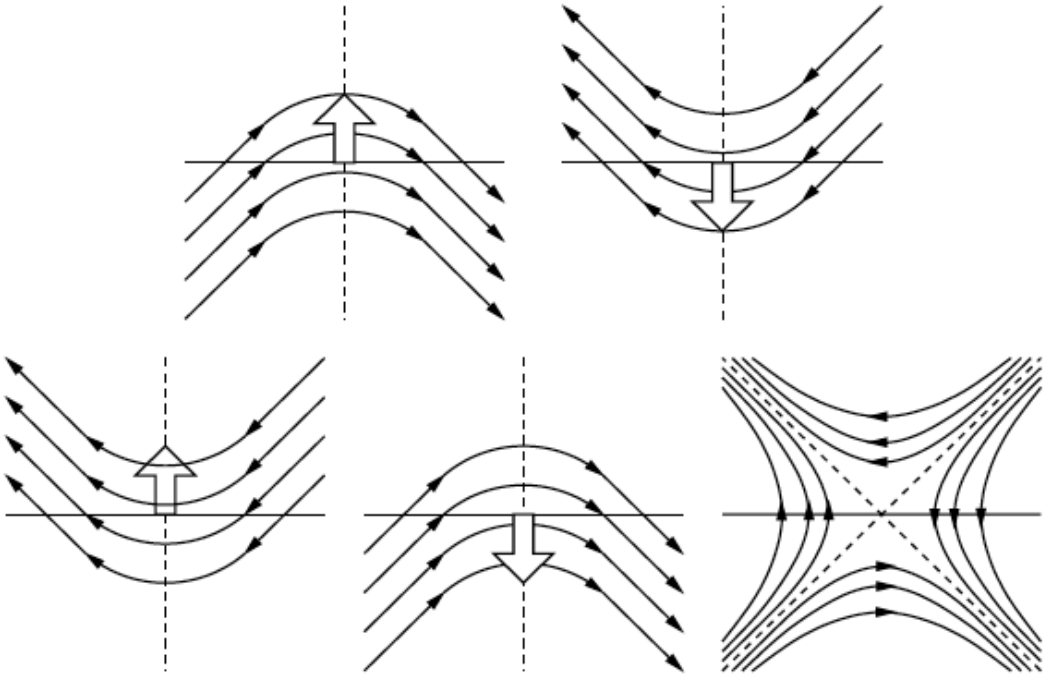

Top: upflows or downflows can lead to flux increases.

Bottom: upflows, downflows, or reconnection can lead to flux decreases

Chae, Moon, & Pevtsov (2004) reported flux submergence in two cancellation events.

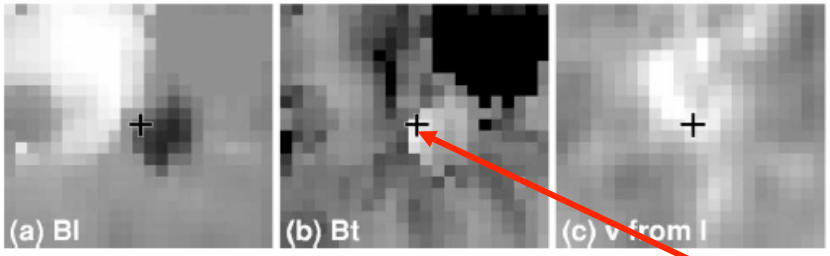

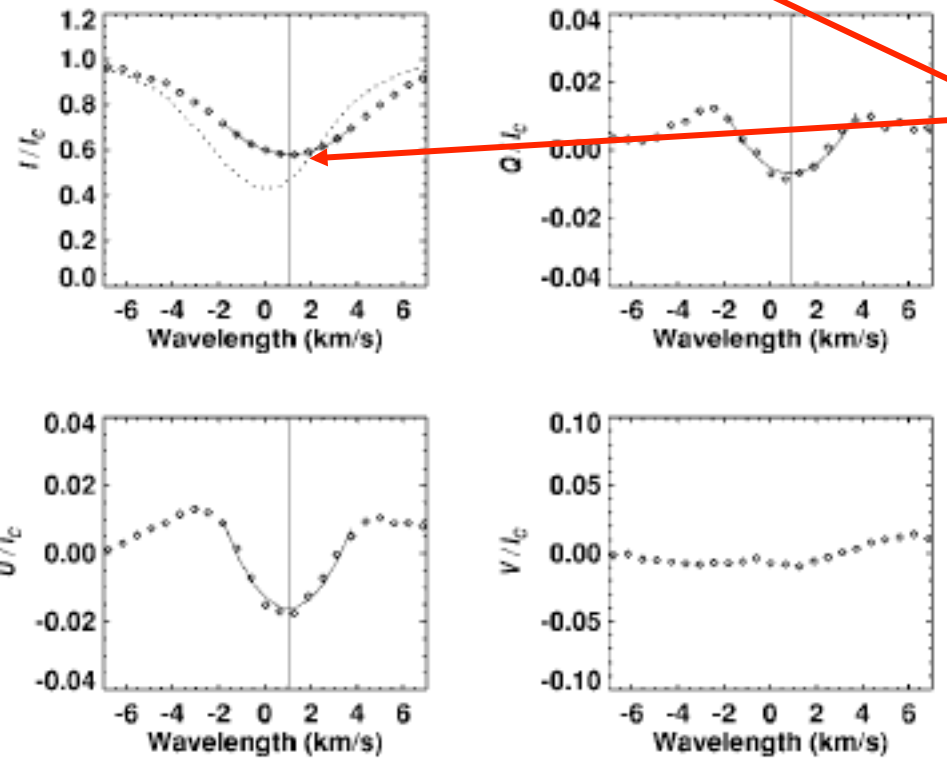

Events were observed with ASP, with pixel scale near 0.''5

They found an ideal electric field: the rate of change of LOS flux matched (v_{Dopp} x B_t) at PIL.

NB: They did not account for the convective blueshift in calibrating the Doppler scale.

But there's a problem with using Doppler velocities directly: the convective blueshift!

From Dravins et al. (1981)

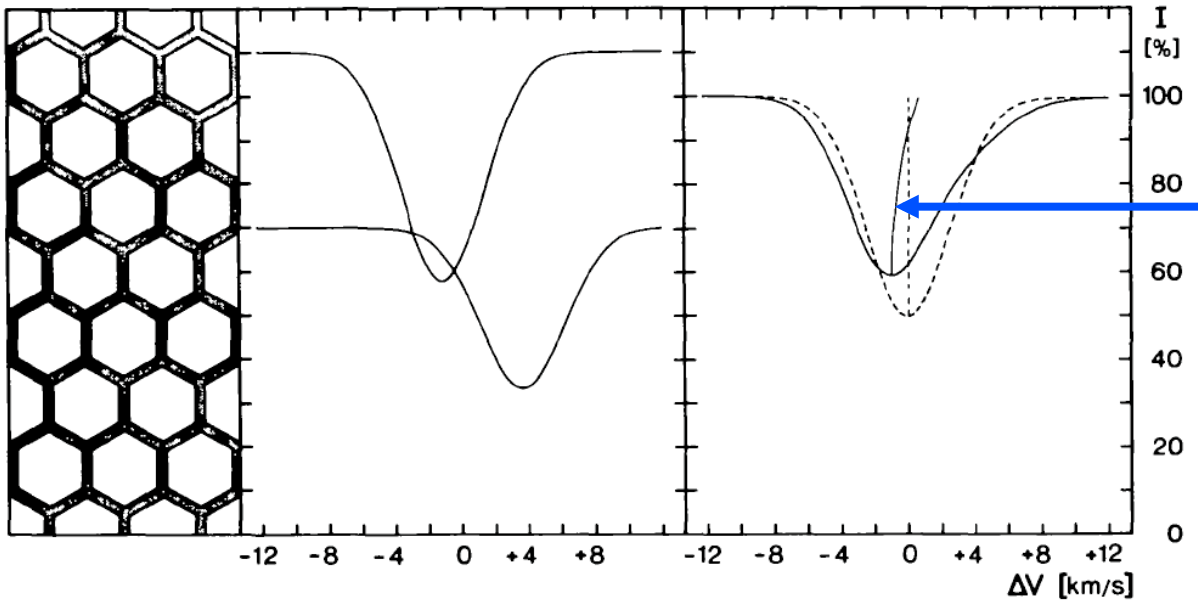

Line "bisector"

Because rising plasma is (1) brighter (it's hotter), and (2) occupies more area, there's an intensity-*blueshift* correlation (talk to P. Scherrer!)

Line center computed from non-magnetized (i.e., strongly convecting) regions will contain this bias!

What if LOS flux cancellation does not match flux transport at PIL? Probable evidence for **non-ideal** evolution.

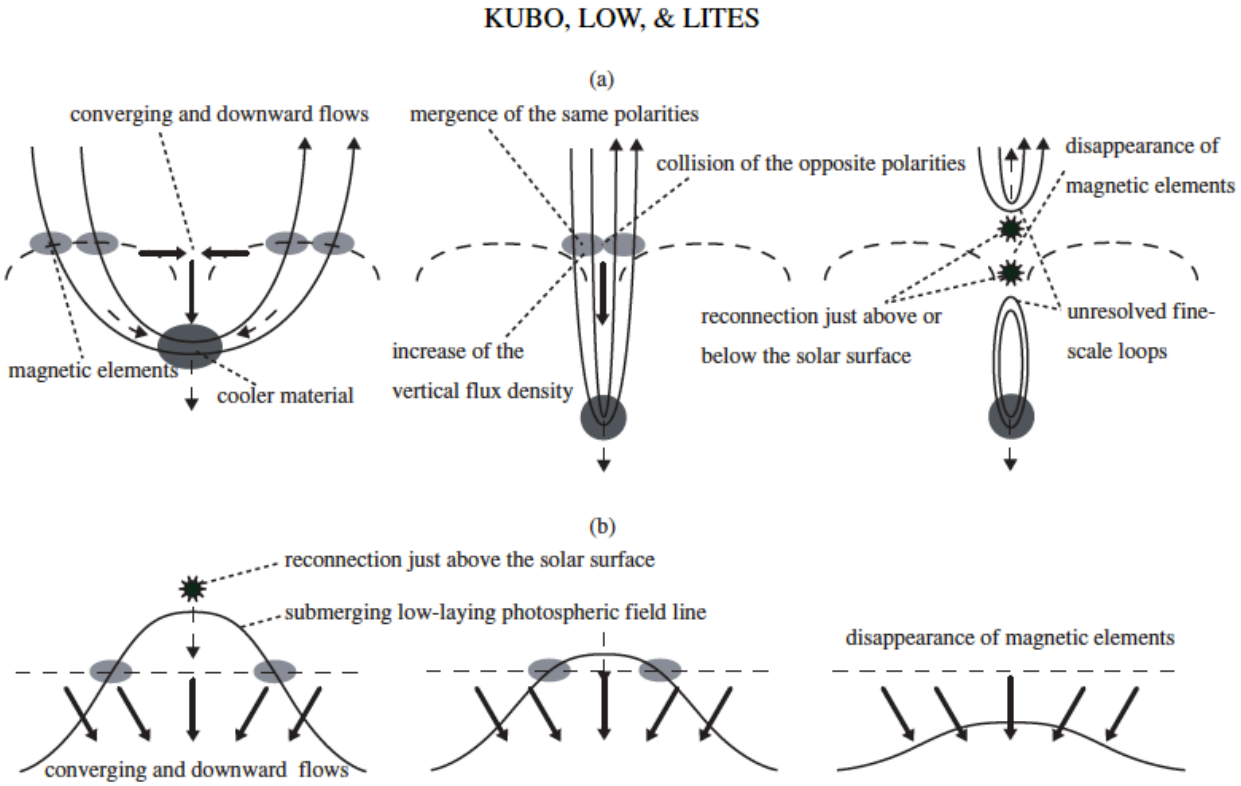

Figure 7. Schematic illustration for a flux cancellation without (panel (a)) and with (panel (b)) the observation of horizontal fields.

Kubo, Low, & Lites (2010) find some cancellations without horizontal field as in top row. "Normal" cancellation is more like bottom row.

Choudhary (SPD poster, 2013) studied Ca II 8542Å Stokes V profiles in SOLIS observations of three ARs.

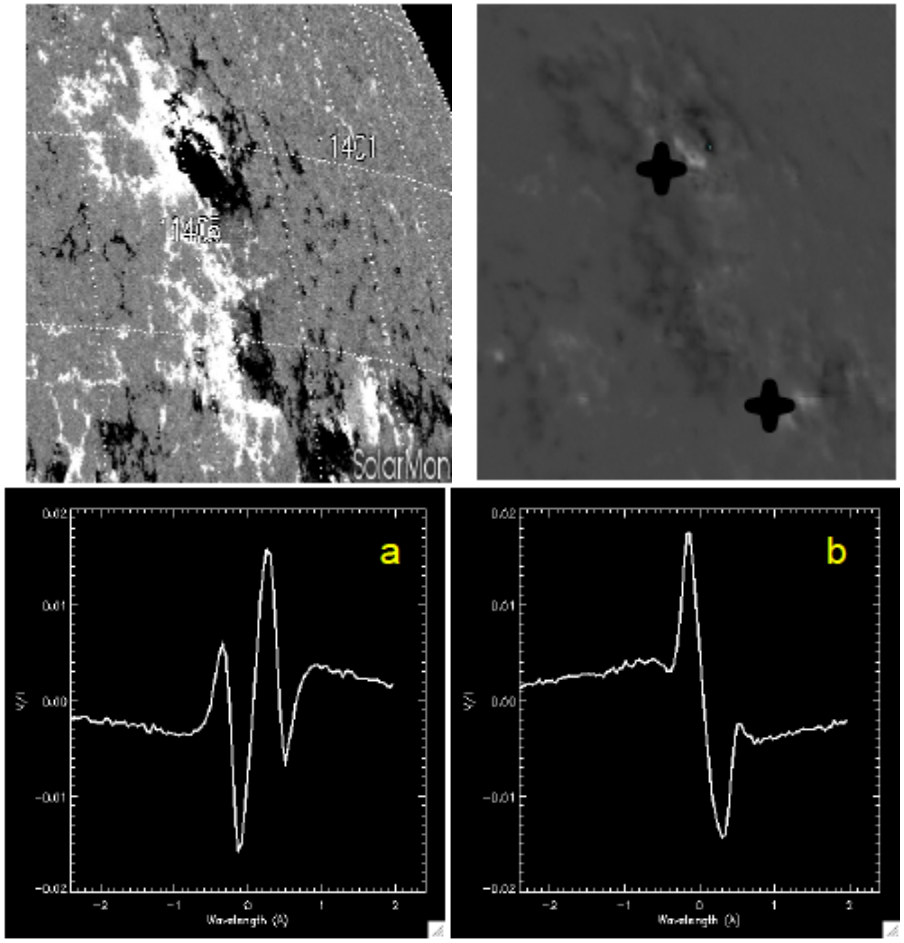

(a) Multiple velocities are sometimes present.

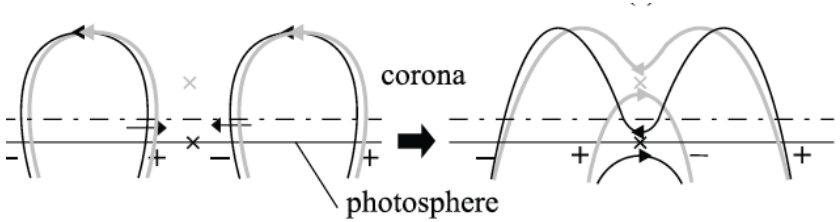

Kubo & Shimizu 2007

(b) Velocities can differ in photosphere & chromosphere (line wing & core).

"…large flares occur when the Stokes-V profiles in [PILs] are more complex with multiple components … and large differential velocities in photosphere and chromosphere."

Welsch et al. (2013) analyzed flux transport by emergence & submergence along ***many*** PILs in AR 11158.

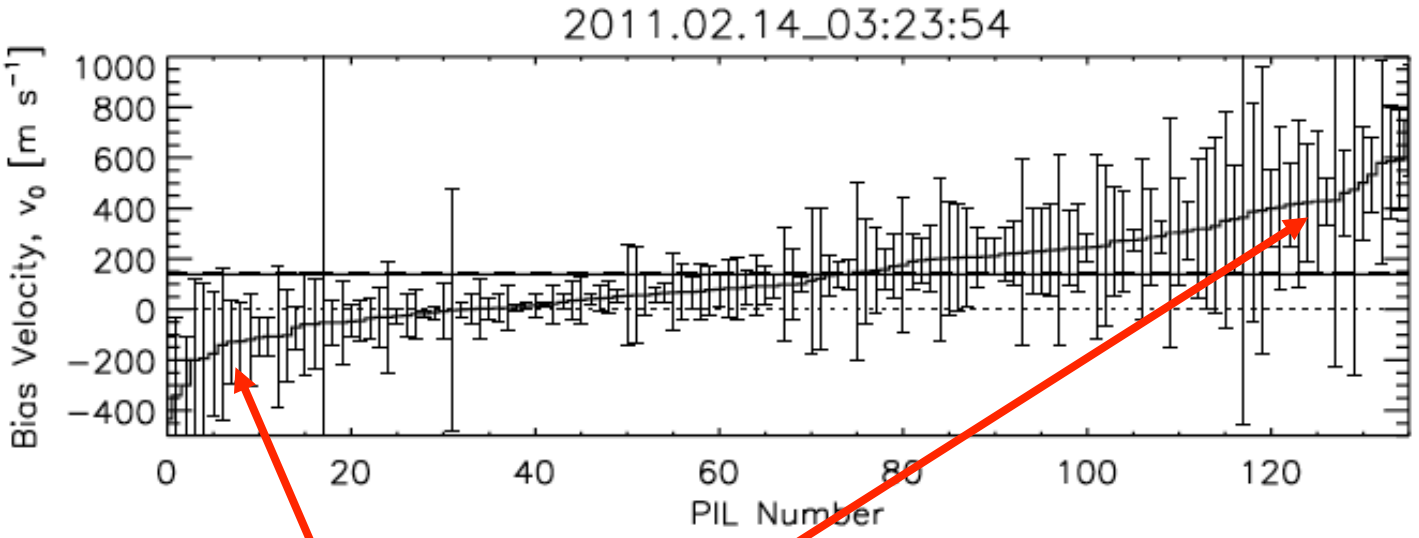

Figure 9. Sorted values of the set of bias velocities, $\{v_0\} = \{\Delta\Phi_{\rm bias}/(\Delta t\,\overline{BL})\}$ from all PILs, (in m s^{-1}) and estimated errors for each PIL (with the astrophysical convention of positive redshift), from three successive (and partially overlapping) magnetogram triplets. The lower thin dotted line shows the (uncalibrated) zero Doppler velocity. The solid and dashed horizontal lines show average and median bias velocities. The magnitudes of the estimated bias velocities are 101 ± 17 m s^{-1}, 126 ± 18 m s^{-1}, and 138 ± 16 m s^{-1}. Only about ~45 of error bars are consistent with each average velocity, suggesting our error estimates are too low, or the ideal assumption is invalid. Nonetheless, our results are consistent with the predominance of redshifts in Figure 6, and indicate that pseudo-redshifts are present.

On some PILs, changes in LOS flux are inconsistent with transport of horizontal fields on PILs.

But this probably arises from ***systematic errors*** in our automated characterization of PILs and neighboring fields.

Conclusion 2: Clearly, higher-resolution studies of dynamics along PILs are needed.

- Higher resolution of Solar-C's SUVIT & ATST could distinguish upflow / downflow regions.

- If evolution is non-ideal, measurement of $\Delta B_h/\Delta z$ enables estimate ***magnetic diffusivity***, η:

$$\Delta\Phi^{(NI)}/\Delta t = L\,\eta\,\Delta B_h/\Delta z$$

Topic 3: In strong flares, photospheric magnetic fields can change "suddenly" and permanently. What's going on?

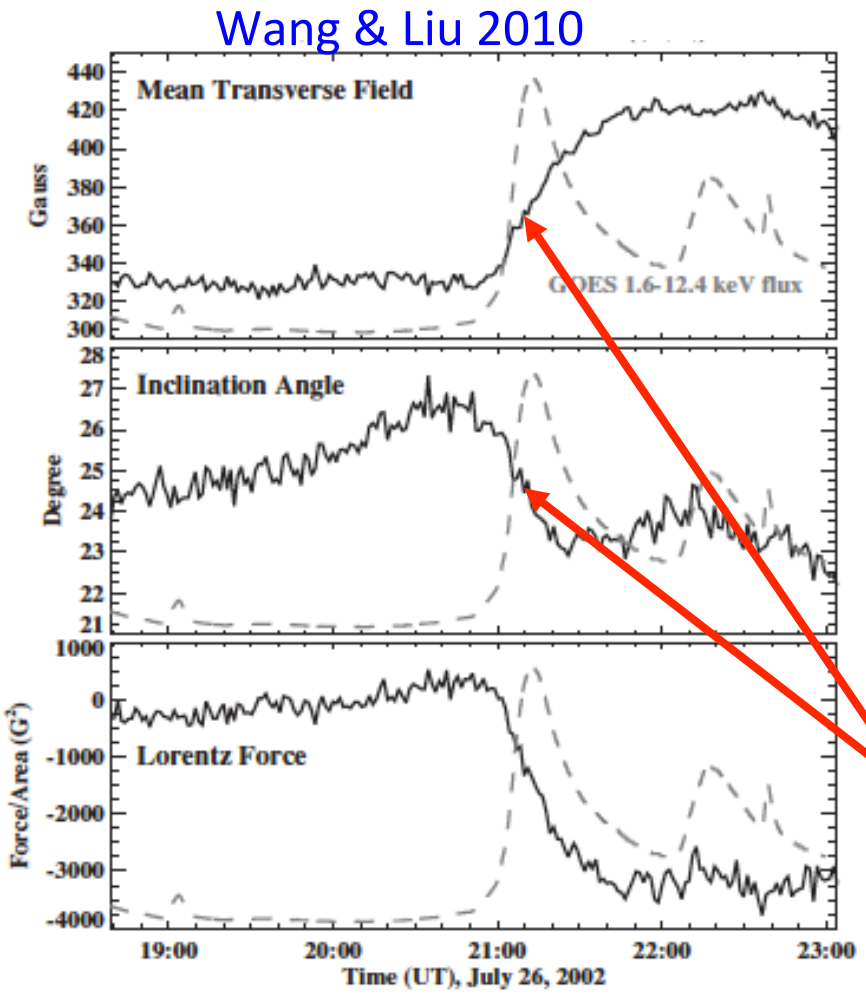

Hudson (2000): coronal fields "implode" in flares and CMEs.

Hudson, Fisher, & Welsch (2008): photospheric **B** should become "**more horizontal**" in flares.

Wang & Liu (2010) find this in many cases!

Q: What processes produce these changes?

What is the mechanism of magnetic field changes?

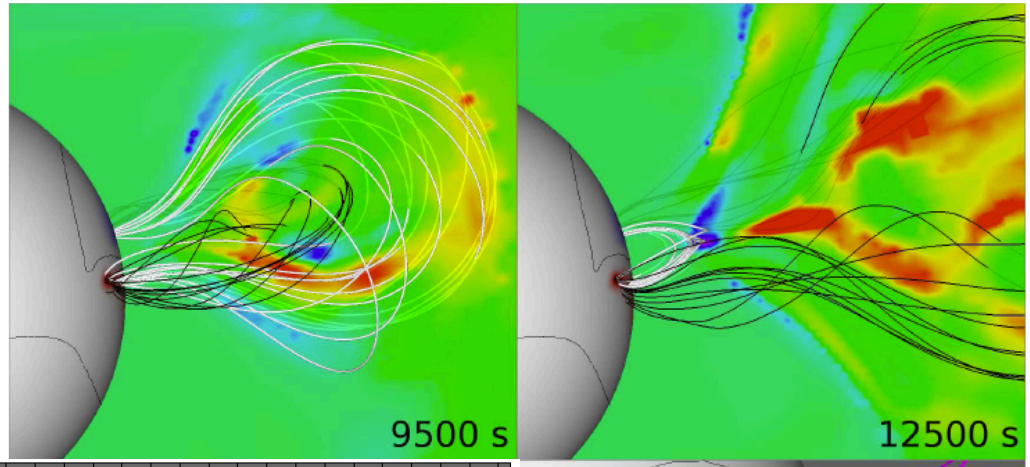

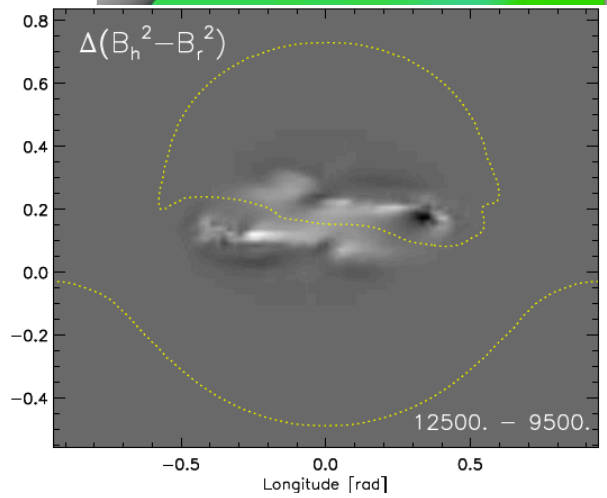

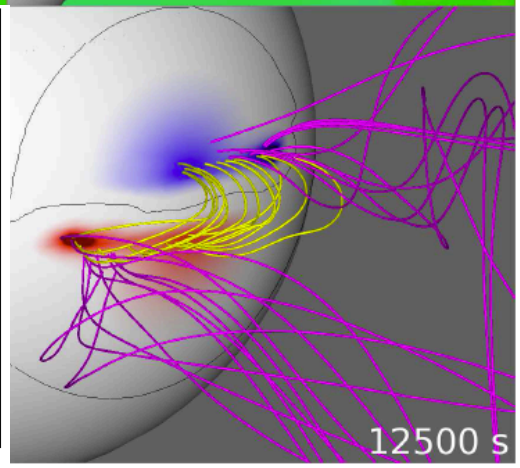

Lorentz force increases beneath PIL!

<u>Hypothesis</u>: increased downward magnetic tension from reconnected loops.

Consistent with "implosion" scenario of Hudson (2000).

ARMS model of CME by Lynch et al. (2009) shows this effect.

Vector magnetograms from HMI during X2.2 flare in AR 11158 show flare-related field changes.

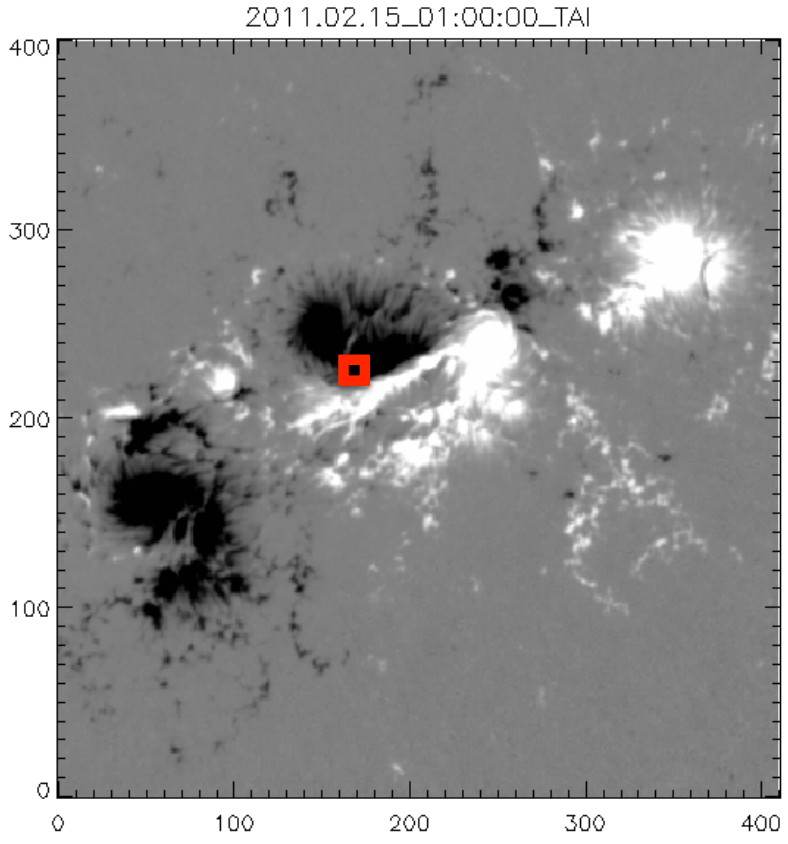

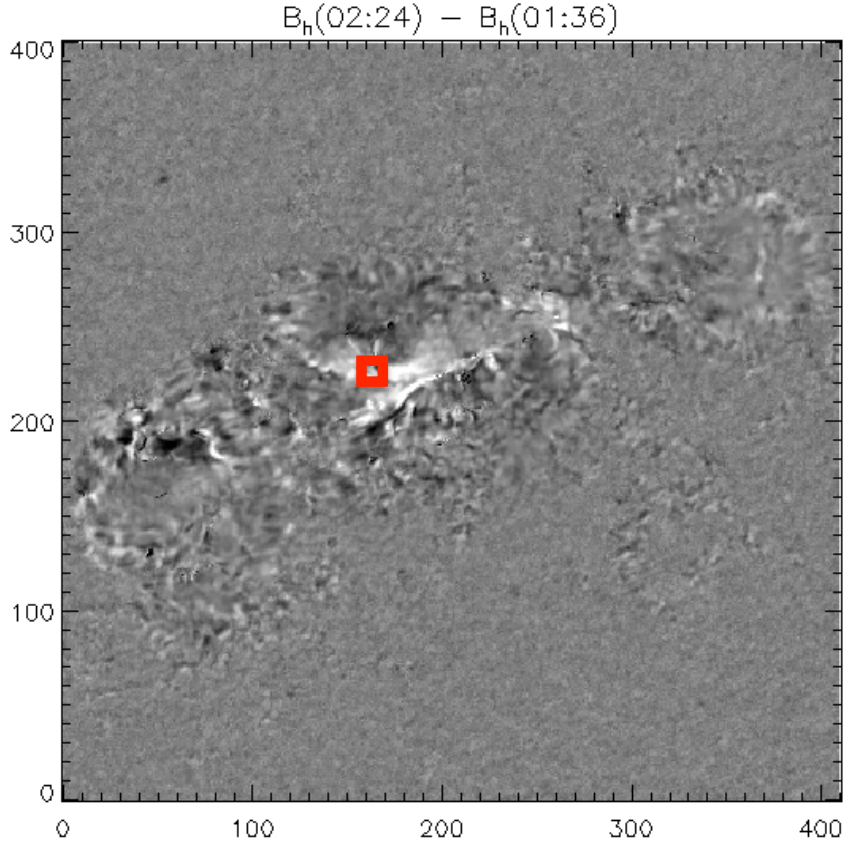

$|\mathbf{B}_h|$ seems to increase in AR cores (under post-flare loops) while $|\mathbf{B}_h|$ decreases toward periphery.

Changes occur ***during*** the flare, in and near sites of flare ribbons. Data cadence is 12 minutes.

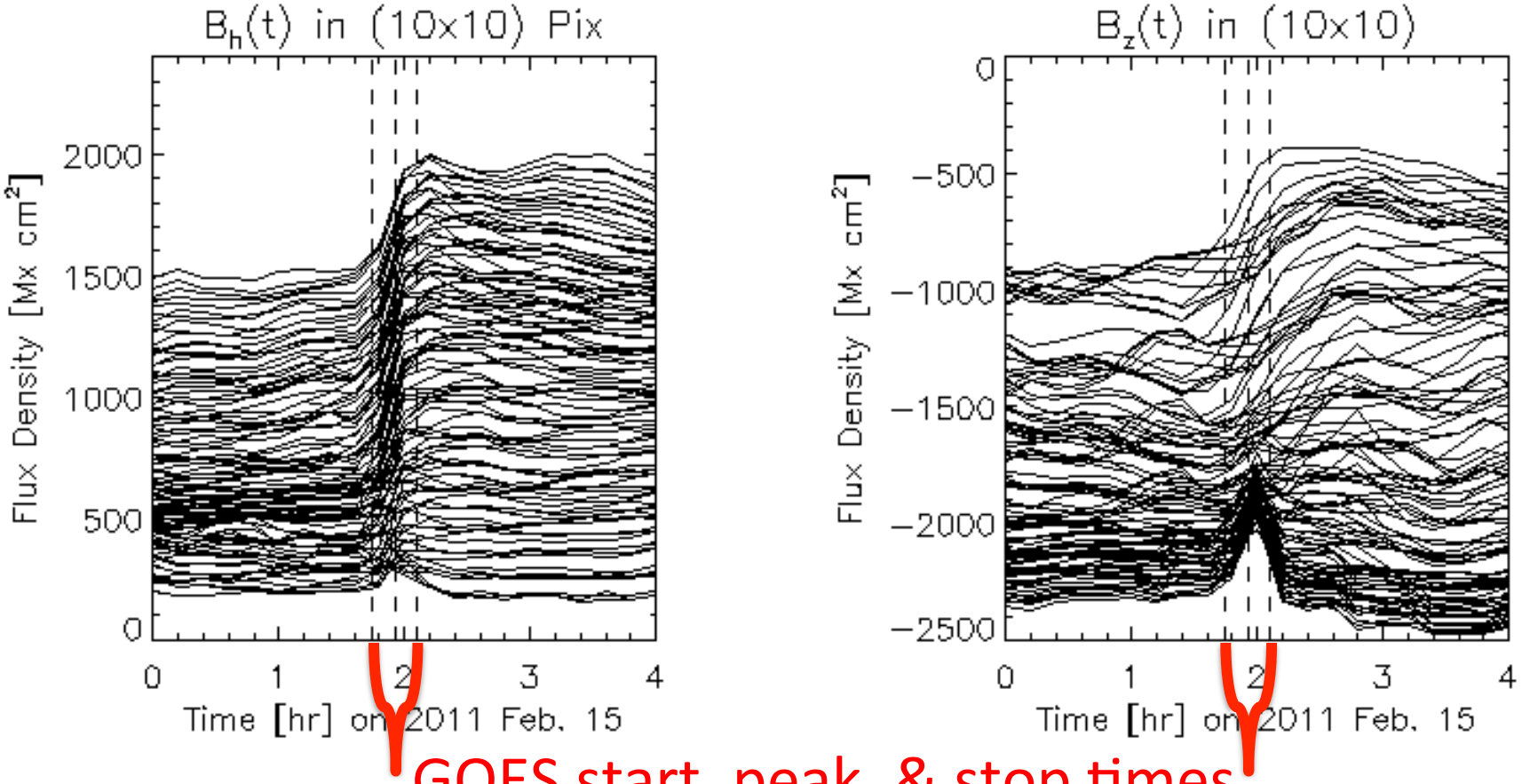

GOES start, peak, & stop times

Charlie Lindsey: spectral line involved in "**criminal activity**"

Difference movie of HMI Dopplergrams shows propagation of changes with ribbons

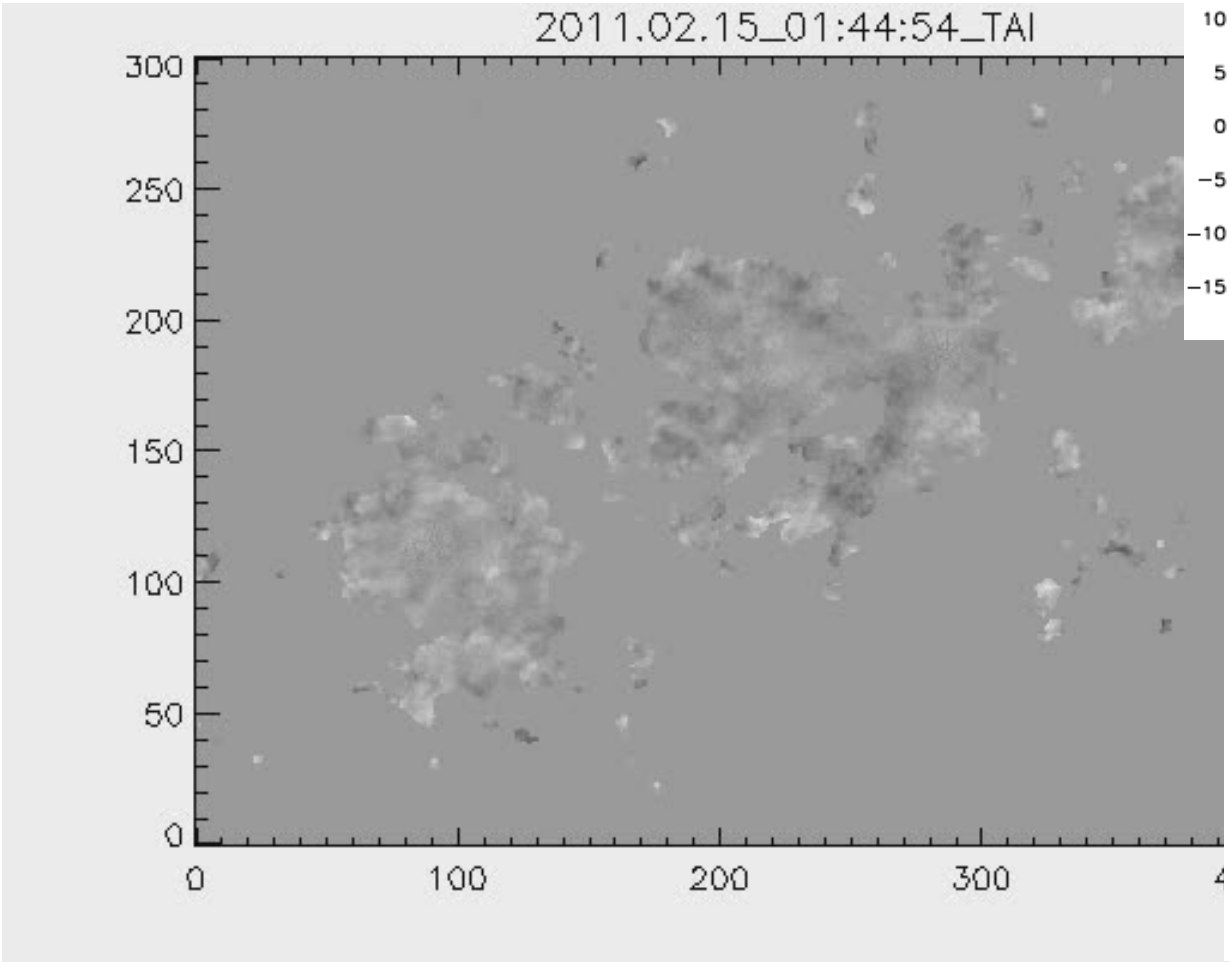

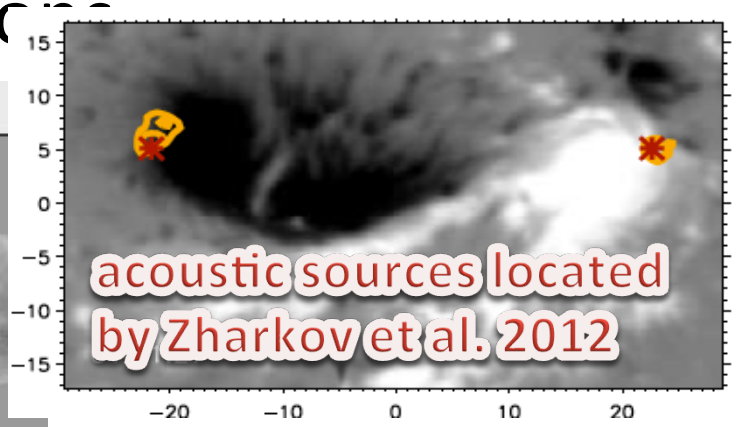

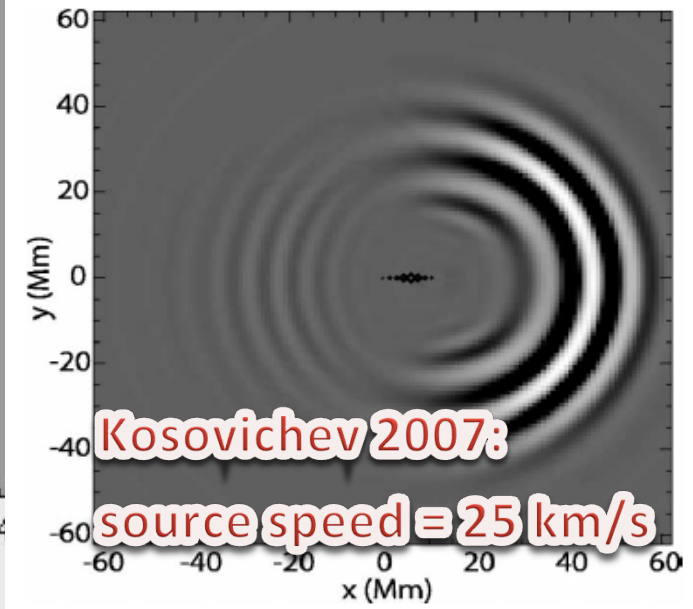

Aside: Do ~1 km/s Doppler "pulses" play any role in Sunquakes?

Ribbon speeds ~20 km/s!

Difference movie of HMI L.o.S. magnetograms shows propagation of changes with ribbons.

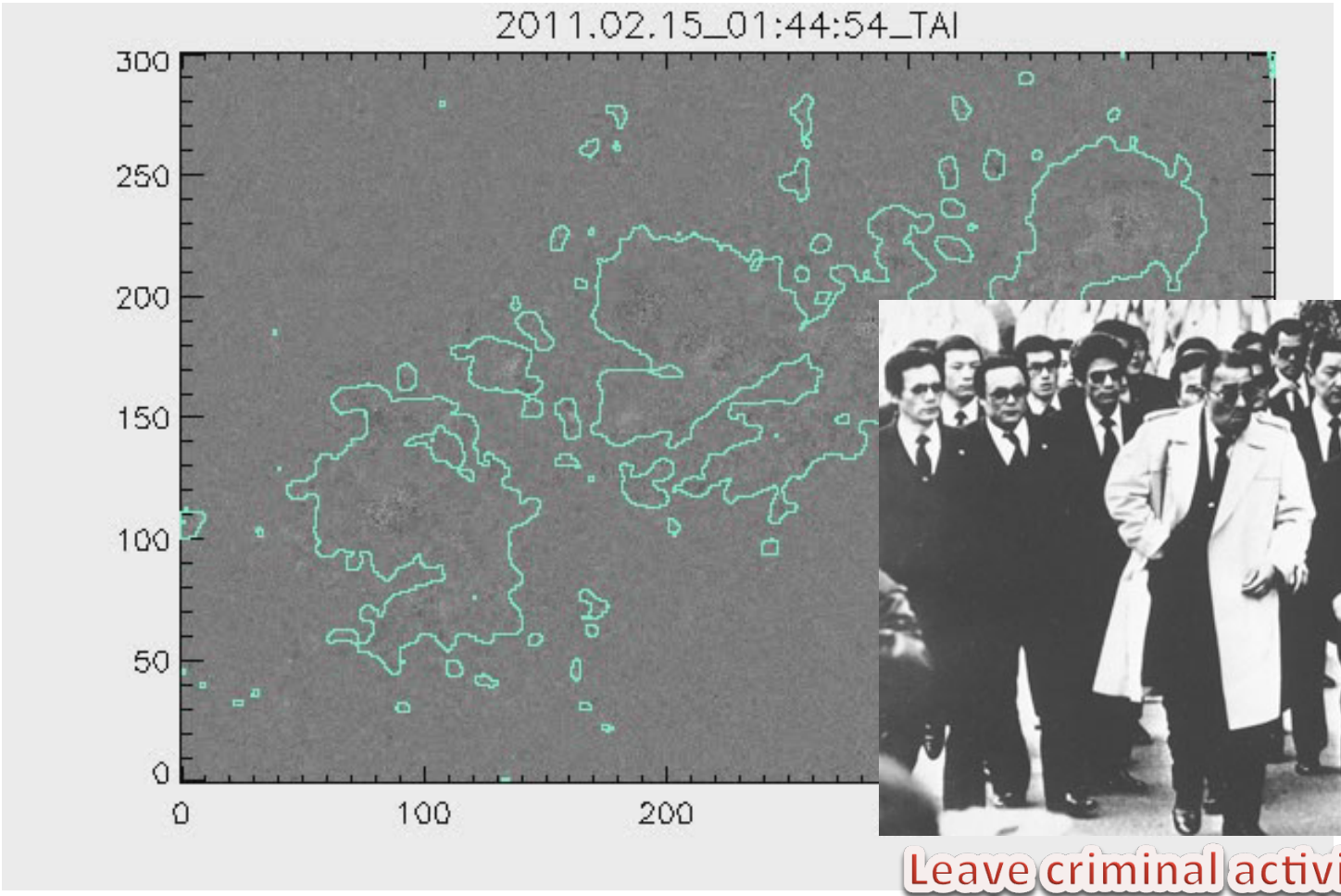

Leave criminal activity to the yakuza?

Again, due to **criminal activity**, these signals probably do not accurately measure changes in $\mathbf{B}_{LoS}$.

Data: HMI's cameras record filtergrams with rapid cadence.

- Each of 2 cameras records an image every 3.75 sec.
- Tunable filter for 6 wavelengths (WL)
  - Internal labels: 465, 467, 469, 471, 473, 475
- Measures 6 polarization states (PS)
  - frame ID 258/258 = LCP/RCP
  - frame ID 250-253 = I,Q,U,V
- Front cam: B_{LOS} (LCP – RCP)* 6 WL repeats in 45 sec, avg'd for 1280 sec
- Side cam: $\boldsymbol{B}$ full-Stokes cycle is 90 sec (4 PS *6 WL), avg'd for 1280 sec

Schou et al., Sol. Phys. **275** 229 (2012)

Table 3 Framelist taking LOS data on the front and full IQUV on the side camera. See text for details.

FID	RelTime	Img	PL	WL	CF	Exp	ObsPath
10098	0	DEFAULT	258	469	DEFAULT	DEFAULT	FRONT2_IMAGE
10090	1875	DEFAULT	250	469	DEFAULT	DEFAULT	SIDE1_IMAGE
10099	3750	DEFAULT	259	469	DEFAULT	DEFAULT	FRONT2_IMAGE
10091	5625	DEFAULT	251	469	DEFAULT	DEFAULT	SIDE1_IMAGE
10079	7500	DEFAULT	259	467	DEFAULT	DEFAULT	FRONT2_IMAGE
10070	9375	DEFAULT	250	467	DEFAULT	DEFAULT	SIDE1_IMAGE
10078	11250	DEFAULT	258	467	DEFAULT	DEFAULT	FRONT2_IMAGE
10071	13125	DEFAULT	251	467	DEFAULT	DEFAULT	SIDE1_IMAGE
10158	15000	DEFAULT	258	475	DEFAULT	DEFAULT	FRONT2_IMAGE
10150	16875	DEFAULT	250	475	DEFAULT	DEFAULT	SIDE1_IMAGE
10159	18750	DEFAULT	259	475	DEFAULT	DEFAULT	FRONT2_IMAGE
10151	20625	DEFAULT	251	475	DEFAULT	DEFAULT	SIDE1_IMAGE
10059	22500	DEFAULT	259	465	DEFAULT	DEFAULT	FRONT2_IMAGE
10050	24375	DEFAULT	250	465	DEFAULT	DEFAULT	SIDE1_IMAGE
10058	26250	DEFAULT	258	465	DEFAULT	DEFAULT	FRONT2_IMAGE
10051	28125	DEFAULT	251	465	DEFAULT	DEFAULT	SIDE1_IMAGE
10138	30000	DEFAULT	258	473	DEFAULT	DEFAULT	FRONT2_IMAGE
10130	31875	DEFAULT	250	473	DEFAULT	DEFAULT	SIDE1_IMAGE
10139	33750	DEFAULT	259	473	DEFAULT	DEFAULT	FRONT2_IMAGE
10131	35625	DEFAULT	251	473	DEFAULT	DEFAULT	SIDE1_IMAGE
10119	37500	DEFAULT	259	471	DEFAULT	DEFAULT	FRONT2_IMAGE
10110	39375	DEFAULT	250	471	DEFAULT	DEFAULT	SIDE1_IMAGE
10118	41250	DEFAULT	258	471	DEFAULT	DEFAULT	FRONT2_IMAGE
10111	43125	DEFAULT	251	471	DEFAULT	DEFAULT	SIDE1_IMAGE
10098	45000	DEFAULT	258	469	DEFAULT	DEFAULT	FRONT2_IMAGE
10092	46875	DEFAULT	252	469	DEFAULT	DEFAULT	SIDE1_IMAGE
10099	48750	DEFAULT	259	469	DEFAULT	DEFAULT	FRONT2_IMAGE
10093	50625	DEFAULT	253	469	DEFAULT	DEFAULT	SIDE1_IMAGE
10079	52500	DEFAULT	259	467	DEFAULT	DEFAULT	FRONT2_IMAGE
10072	54375	DEFAULT	252	467	DEFAULT	DEFAULT	SIDE1_IMAGE
10078	56250	DEFAULT	258	467	DEFAULT	DEFAULT	FRONT2_IMAGE
10073	58125	DEFAULT	253	467	DEFAULT	DEFAULT	SIDE1_IMAGE
10158	60000	DEFAULT	258	475	DEFAULT	DEFAULT	FRONT2_IMAGE
10152	61875	DEFAULT	252	475	DEFAULT	DEFAULT	SIDE1_IMAGE
10159	63750	DEFAULT	259	475	DEFAULT	DEFAULT	FRONT2_IMAGE
10153	65625	DEFAULT	253	475	DEFAULT	DEFAULT	SIDE1_IMAGE
10059	67500	DEFAULT	259	465	DEFAULT	DEFAULT	FRONT2_IMAGE
10052	69375	DEFAULT	252	465	DEFAULT	DEFAULT	SIDE1_IMAGE
10058	71250	DEFAULT	258	465	DEFAULT	DEFAULT	FRONT2_IMAGE
10053	73125	DEFAULT	253	465	DEFAULT	DEFAULT	SIDE1_IMAGE
10138	75000	DEFAULT	258	473	DEFAULT	DEFAULT	FRONT2_IMAGE
10132	76875	DEFAULT	252	473	DEFAULT	DEFAULT	SIDE1_IMAGE
10139	78750	DEFAULT	259	473	DEFAULT	DEFAULT	FRONT2_IMAGE
10133	80625	DEFAULT	253	473	DEFAULT	DEFAULT	SIDE1_IMAGE
10119	82500	DEFAULT	259	471	DEFAULT	DEFAULT	FRONT2_IMAGE
10112	84375	DEFAULT	252	471	DEFAULT	DEFAULT	SIDE1_IMAGE
10118	86250	DEFAULT	258	471	DEFAULT	DEFAULT	FRONT2_IMAGE
10113	88125	DEFAULT	253	471	DEFAULT	DEFAULT	SIDE1_IMAGE

Single-WL Stokes $V(x,y)$ signal clearly shows magnetic structure at a given time.

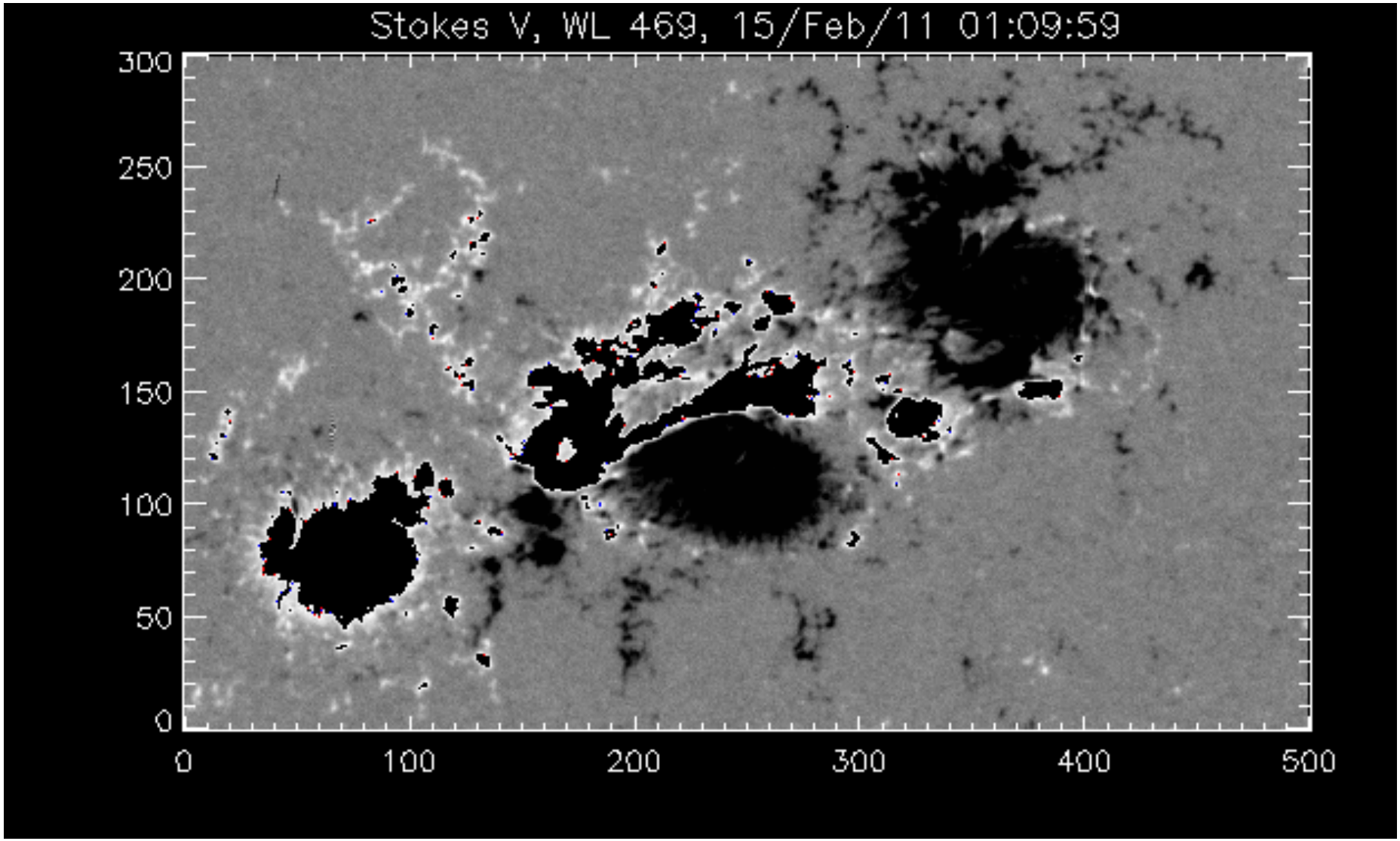

Pixel time profiles in single-λ HMI filtergrams can be fitted as Sudol & Harvey (2005), but here also with a t^2 term.

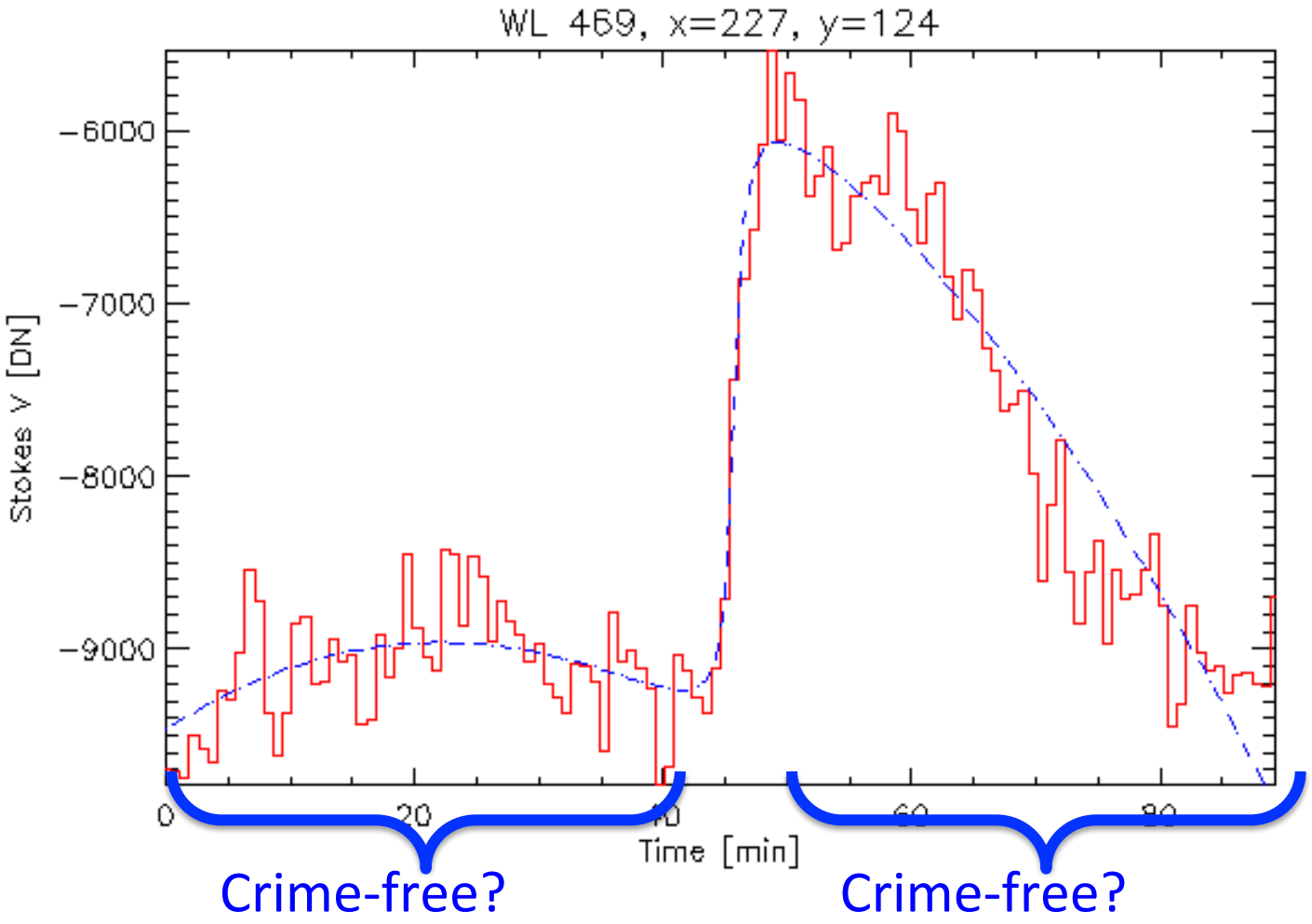

Changes in this pixel are resolved at 45 sec cadence! $\Delta t \sim$ 4 min.

Among single-WL fits, the distribution of fitted timescales is consistent with field changes over a few sec.

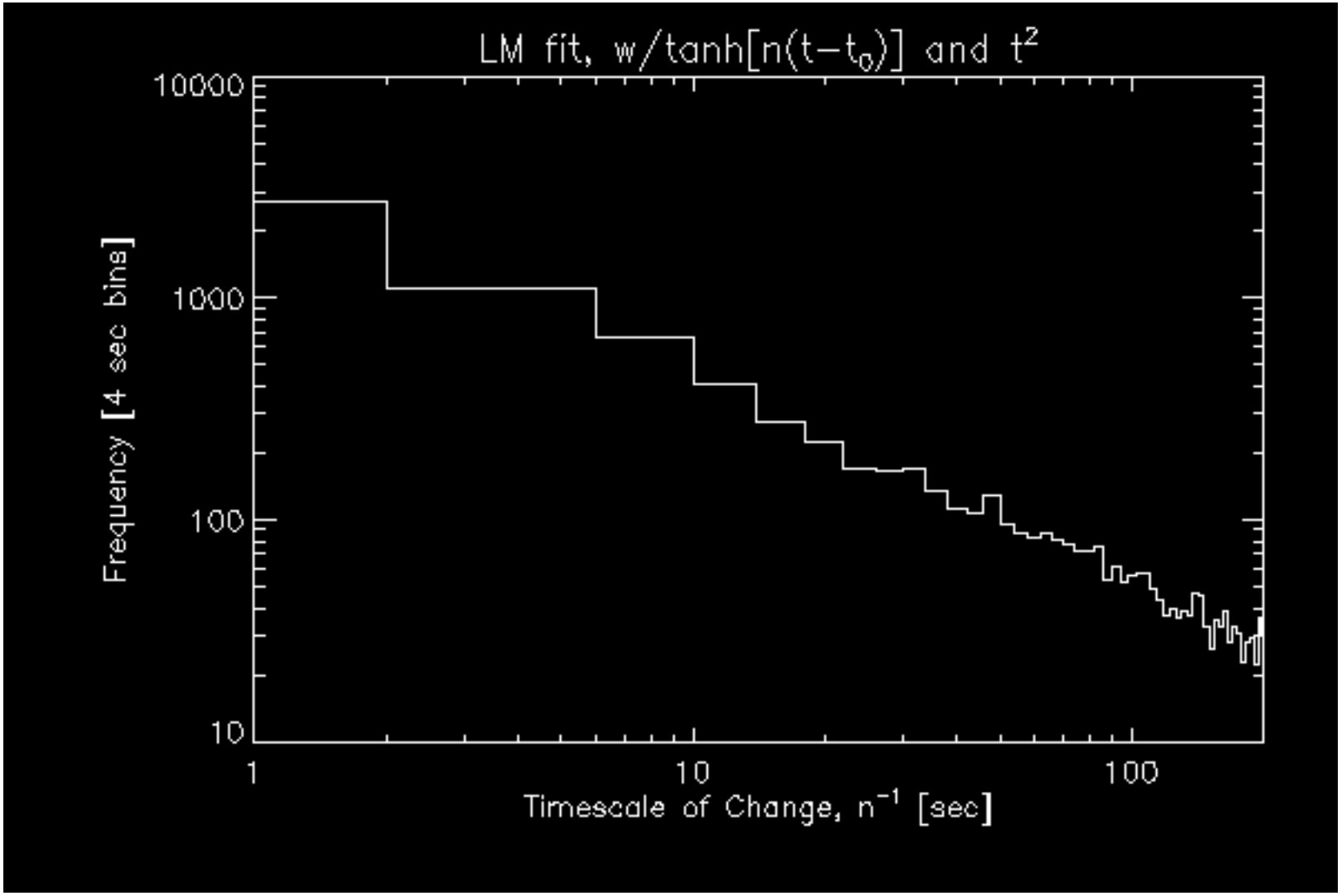

Johnstone et al. (2012) showed that magnetic field changes in GONG lagged UV ribbon emission from TRACE.

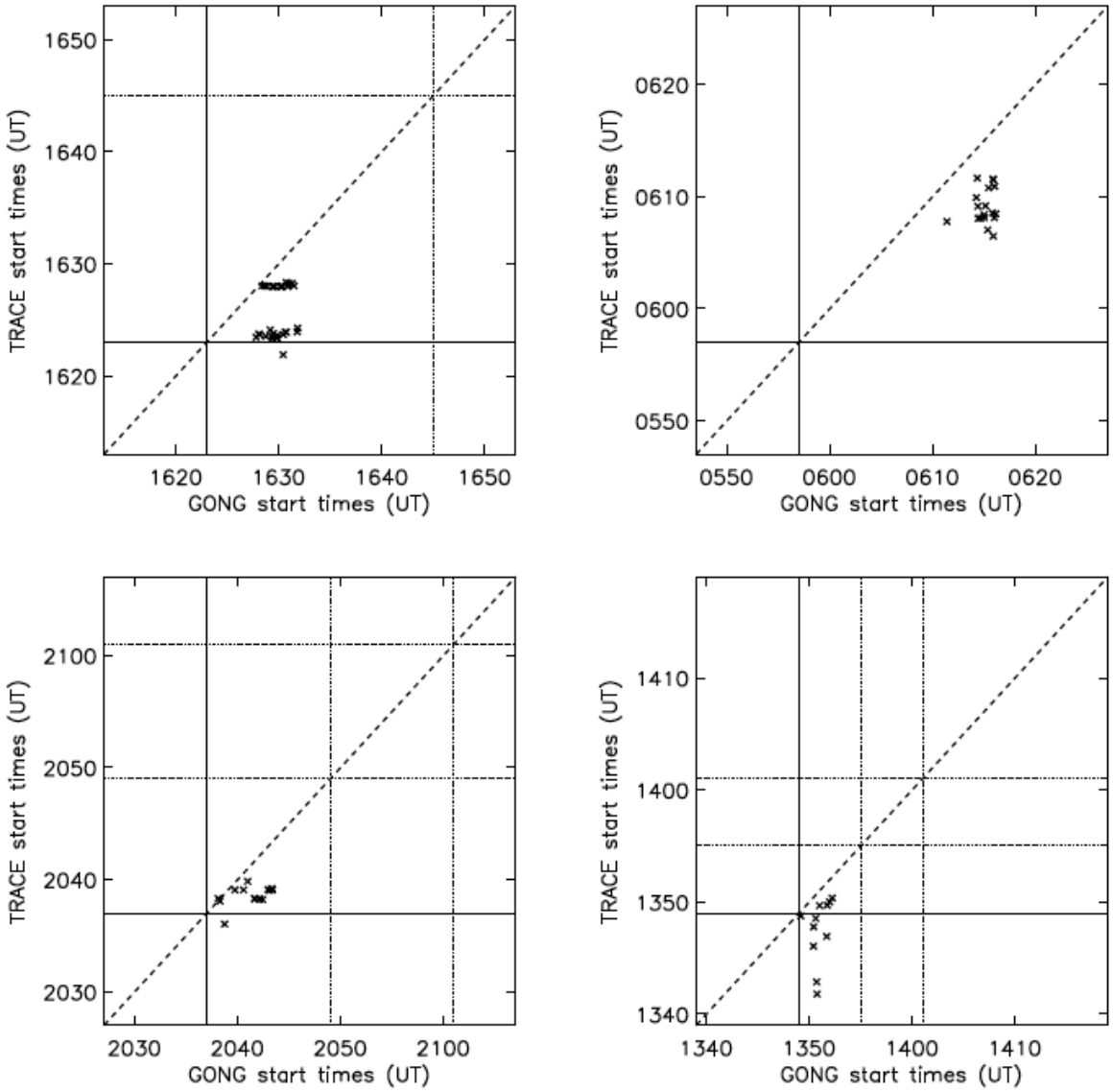

They found GONG lags in all 4 flares in their sample.

UV emission persisted for much longer than the timescale of field changes.

Observational goals: Estimate **v** & **E** from flare-driven Δ**B** to investigate dynamics & Poynting flux.

- **B**(t_{pre}) & **B**(t_{post}) must **crime-free** measurements.
- Cadence Δt must be rapid enough that field does not change (much) from convection.
- Measurements of flare-driven changes, Δ**B**, in the chromosphere (and corona!) would be very helpful.
- Detailed spectral information might enable investigating criminal activity…

Conclusion 3: High-resolution, high-cadence studies of magnetic evolution in flare sites are needed.

- Spatial scales of flare ribbon emission (associated with permanent field changes) are likely currently unresolved.

- Important to catch changes in **B**, requiring **high cadence** vector magnetograms

==> photons needed! Solar-C's 1.4 m aperture is **essential!**

- High-duty-cycle of spaceborne magnetographs should improve odds of catching flares compared to ground-based instruments.

Overall Conclusions

- Studies of photospheric velocities can reveal crucial aspects of key physical processes in several areas of solar physics.

- In several research areas, studies with higher resolution in space and time are crucial to improving our understanding.

A copy of this talk is at
http://solarmuri.ssl.berkeley.edu/~welsch/public/presentations/Hinode7/welsch_hinode7.pptx